1 Long-term PM trends at boreal forest site in southern Finland from three different

2 measurement techniques

3

- 4 Ilona Ylivinkka^{1,2}, Helmi-Marja Keskinen¹, Lauri R. Ahonen^{1,2}, Liine Heikkinen^{1,3,4}, Pasi P.
- 5 Aalto¹, Tuomo Nieminen^{1,5}, Katrianne Lehtipalo^{1,6}, Krista Luoma^{1,6}, Sujai Banerji¹, Juho
- 6 Aalto^{2,7}, Janne Levula¹, Jutta Kesti^{1,6}, Ekaterina Ezhova¹, Markku Kulmala¹, and Tuukka
- 7 Petäjä¹

- 9 ¹Institute for Atmospheric and Earth System Research (INAR) / Physics, Faculty of Science,
- 10 University of Helsinki, Helsinki, 00014, Finland
- 11 ²Station for Measuring Ecosystem Atmosphere Relations II (SMEAR II), University of
- 12 Helsinki, Korkeakoski, 35500, Finland
- 13 ³Department of Environmental Science, Stockholm University, Sweden
- 14 ⁴Bolin Centre for Climate Research, Stockholm University, Sweden
- 15 Department of Physics, Faculty of Science, University of Helsinki, Finland
- 16 ⁶Finnish Meteorological Institute, 00560 Helsinki, Finland
- 17 Institute for Atmospheric and Earth System Research (INAR) / Forest Sciences, Faculty of
- 18 Agriculture and Forestry, University of Helsinki, Helsinki, 00014, Finland
- 19 *Correspondence to*: Ilona Ylivinkka (ilona.ylivinkka@helsinki.fi)
- 20 **Abstract.** Three independent particulate matter (PM) mass concentration measurements and
- 21 their long-term (2005–2020) trends were compared at the Station for Measuring Ecosystem–
- 22 Atmosphere Relations (SMEAR II, Hyytiälä, Finland). The different methods (gravimetric
- 23 method with a cascade impactor, Synchronized Hybrid Ambient Real-time Particulate
- 24 Monitor (SHARP; only PM₁₀), and calculated PM concentration from combined Differential
- 25 Mobility Particle Sizer (DMPS) and Aerosol Particle Sizer (APS) particle number size
- 26 distribution data) showed good correlation (Pearson's correlation coefficient approximately
- 27 0.8) in all size classes (PM₁, PM_{2.5} and PM₁₀). The mass concentrations in all PM classes
- 28 were the highest in summer and the lowest in autumn and winter. Statistically significant
- 29 (Mann–Kendall test) declining annual trends were observed in DMPS+APS and impactor
- data in all size classes, ranging from -0.021 to -0.036 µg m⁻³ y⁻¹. While DMPS+APS method
- 31 indicated statistically significant decline also in all seasons, the decline in impactor data was
- 32 statistically significant only in spring and winter. SHARP data could not be used for trend
- estimation due to the change in inlet heating temperature, affecting the measured PM₁₀

concentrations. Seasonally, the decline was smallest in summer, which follows the trends observed also in SO₂ and NO_x concentrations. The results underline both the summertime dominance of biogenic sources for the aerosol mass concentration in the rural boreal forest environment and the reduction of anthropogenic pollution due to the EU level restrictions for improved air quality.

39

40

34

35

36

37

38

1 Introduction

41 Particulate matter (PM) concentrations are monitored worldwide, because they are connected 42 to health effects, such as asthma and cardiovascular diseases, and premature deaths (Pope et 43 al., 2003; Shiraiwa et al., 2017; WHO, 2021). The increased knowledge regarding the 44 relationship between air pollution and mortality have resulted in air pollution regulations, 45 which additionally aim to decrease inequality related to air pollution exposure (Wang et al., 2017; WHO, 2021). Besides the adverse health effects, aerosol particles can also scatter or 46 absorb radiation and participate in cloud formation and processing, thus affecting the Earth's 47 48 climate (IPCC, 2021). While the overall effect of aerosol particles on climate is considered to 49 be cooling, radiative forcing due to aerosol particles and especially due to aerosol-cloud-50 radiation interactions is uncertain (IPCC, 2021). 51 52 PM measurements are divided into size classes based on the aerodynamic diameter of the 53 particles: PM₁, PM_{2.5}, and PM₁₀ with upper maximum diameters of particles 1 μm, 2.5 μm, 54 and 10 µm, respectively. The PM mass concentration in these classes is the total mass of 55 particles below the limiting size. The size of aerosol particles is a critical parameter, both in 56 terms of their climate (e.g., Pöschl, 2005; Dusek et al., 2006) and health effects 57 (Schraufnagel, 2020). In principle, the smaller the particles are, the deeper they can penetrate 58 in the human respiratory system and thus end up also in other organs than lungs (Pope et al., 59 2003; Maynard & Kuempel, 2005). The smallest particles have only a minor contribution to the aerosol mass concentration, but they dominate the particle number concentration. In 60 61 climate perspective, the most relevant particles are larger than about 50–100 nm, since those 62 can act as cloud condensation nuclei as well as scatter or absorb radiation (IPCC, 2021).

64 Aerosol particles have both natural and anthropogenic sources. Additionally, particles can be 65 transported over hundreds or thousands of kilometers, since the lifetime of PM in the 66 atmosphere is days to weeks, depending on the size, composition, and source region of the 67 particles (Seinfeld and Pandis, 2006; Manavi et al., 2025). Primary aerosol particles consist 68 mostly of particles from traffic and industry (e.g., black carbon (BC)), or from natural sources 69 (e.g., volcanic ash, sea-spray, dust, and pollen), and they contribute to all PM classes. 70 Secondary aerosol particles are formed in the atmosphere from gas-phase precursor vapors 71 (e.g. Kulmala et al., 2013). These particles eventually grow to larger sizes, contributing 72 particularly to the accumulation mode, and thereby to PM₁. 73 74 At SMEAR II, organic aerosol (OA) from oxidized biogenic volatile organic compounds (VOCs), most importantly monoterpenes from the surrounding forest (Rinne et al., 2005), is 75 76 the most abundant PM₁ component (Jimenez et al., 2009; Heikkinen et al., 2020). The 77 emission rates of monoterpenes are boosted by warm temperatures (Guenther et al., 1993), 78 which is also observed in the OA mass concentrations (Heikkinen et al., 2021; Yli-Juuti et al., 79 2021). Sulfate, another key PM₁ component at SMEAR II and globally, is formed, e.g., upon 80 oxidation from sulfur dioxide (SO₂), mostly emitted by industry (Seinfeld and Pandis, 2006). 81 Nitrate aerosol mass concentrations, mostly prevalent in agricultural or urban environments, 82 are therefore less abundant at SMEAR II (Makkonen et al., 2014). 83 84 The European Union has regulated the exposure on air pollution since 2005 via air quality 85 directives (https://environment.ec.europa.eu/topics/air/air-quality/eu-air-quality-standards_en; 86 accessed: 31 Jul 2025). The air quality directives concern basic pollutants: PM, trace gases 87 (SO₂, NO₂, O₃, CO, benzene, and polyaromatic hydrocarbons) as well as heavy metals (Pb, As, Ni, and Cd). Originally legislation on PM concerned only PM₁₀ concentration (yearly 88 average concentration was limited to 40 µg m⁻³), but in 2010 target value was set for PM_{2.5} 89 concentration (25 µg m⁻³ and limited to 20 µg m⁻³ in 2020). 90 91 92 In the end on 2024, The Ambient Air Quality Directive was revised (2024/2881), forcing 93 further reductions for targets values of many pollutants, including PM₁₀, PM_{2.5}, O₃, SO₂, CO, 94 and benzene. Additionally, the new air quality directive introduces advanced measurement 95 parameters, such as aerosol number concentration, aerosol size distribution, BC, and 96 oxidative potential, to address i.a. the harmfulness of small aerosol particles. Air quality

supersite concept was implemented as well (Kuula et al., 2021), aiming to compare the health

98 impacts of the ultrafine particles and PM_{2.5} in urban and rural supersites. In addition, the EU 99 Commission mandates measurements of ultrafine (defined as particles between 10 to 100 nm 100 in diameter) and BC concentrations in the vicinity of air pollution hotspots. 101 102 Several studies have already reported declining PM concentrations in Europe (Barmpadimos 103 et al., 2011; 2012; Cusack et al., 2012; Pandolfi et al., 2016), ranging approximately from -104 0.008 PM_{2.5} trend in Po Valley, Italy (Bigi & Ghermandi, 2016) to -4.11 µg m⁻³ yr⁻¹ in (sub)urban Germany (Guerreiro et al., 2014). In some cases, also increasing trends have also 105 106 been measured in relation to increased emissions from, for example, household combustion and agriculture (Guerreiro et al., 2014). Declining trends are related to the legislation on air 107 quality as well as improved technology in industry, traffic, and heating (Spindler et al., 2004; 108 Anttila & Tuovinen, 2010; Barmpadimos et al., 2011; Cusack et al., 2012; Keuken et al., 109 110 2012). In Finland, the PM concentrations have been declining during the past decades and 111 generally are well below the limit values (Laakso et al., 2003; Anttila, 2020). 112 113 Techniques for measuring aerosol mass concentrations have improved remarkably during the 114 last decades (Van Dingenen et al., 2004; Occhipinti & Oluwasanya, 2017; Shukla & 115 Aggarwal, 2022). Most of the PM measurements have traditionally been done by offline 116 gravimetric analyses where particle size classes are separated, e.g., by impactor (Laakso et 117 al., 2003) or special high-volume samplers (Barmpadimos et al., 2011). The offline methods are quite laborious as their sampling time is up to few days and weighing is done manually. 118 119 Thus, PM concentrations are nowadays more commonly measured with online techniques, 120 such as tapered element oscillating microbalance (TEOM) with the Continuous Ambient 121 Particulate Monitor and Synchronized Hybrid Ambient Real-time Particulate monitor 122 (SHARP) (Laakso et al., 2008; Chen et al., 2018, Waldén et al., 2010). Besides the direct 123 mass measurements, the particle mass can be calculated from the particle number size distribution with assumptions regarding particles' shape and density (Neusüß et al., 2000). 124 125 The aim of this work is threefold. First, we compare the PM concentrations obtained from 126 127 gravimetric impactor, online mass analyzer SHARP and from the particle number size 128 distribution to explore their applicability for continuous PM measurements. Second, we report for the first time long-term (2005–2020) measurements of PM₁₀, PM_{2.5} and PM₁ at 129 SMEAR II, Finland, and explore the overall concentration levels as well as selected specific 130 episodes. Third, we estimate the trends of the PM concentrations separately for each season 131

132 and the impact of the EU legislation on the PM trends. Quality controlled data on aerosol 133 particle mass concentration in a boreal background station enable us to explore the role of local, regional and global phenomena controlling the aerosol mass concentration in the 134 region. This work continues the analysis presented in Keskinen et al. (2020) with updated 135 datasets and revised analysis methods. 136 137 2 Methods 138 2.1 Measurement station 139 The measurements were performed at SMEAR II, located in Hyytiälä in southern Finland 140 (61°51'N, 24°17'E; 181 m a.s.l.; Fig. 1a). Hyytiälä is a rural background measurement site 141 with low local anthropogenic emissions (Hari and Kulmala, 2005). A photo of the 142 homogeneous 60-year-old Scots pine stand surrounding SMEAR II is presented in Fig. 1c. 143 The nearest cities are Tampere (50 km southwest; 249 000 inhabitants) and Jyväskylä (90 km 144 northeast; 146 000 inhabitants). 145 146 The station is equipped with instruments for continuous and comprehensive measurements of 147 interactions between the forest ecosystem and atmosphere (Hari and Kulmala et al., 2005). 148 SMEAR II is part of the European Aerosols, Clouds, and Trace gases Research Infrastructure 149 (ACTRIS; Laj et al. 2024; https://www.actris.eu/, accessed 07 Aug 2025). The presented 150 measurements are conducted inside the canopy with total suspended particulates (TSP) or PM₁₀ design inlets for the different aerosol measurements on the roof of the aerosol cottage 151 (Fig. 1b). Winter at SMEAR II is defined to be from December to February (DJF), spring is 152 from March to May (MAM), summer from June to August (JJA) and autumn from September 153 to November (SON). Note that winter has January and February data from the following year. 154 155 Due to the data availability, measurements start from spring 2005 and in the end of the measurement period winter includes only December 2020. 156

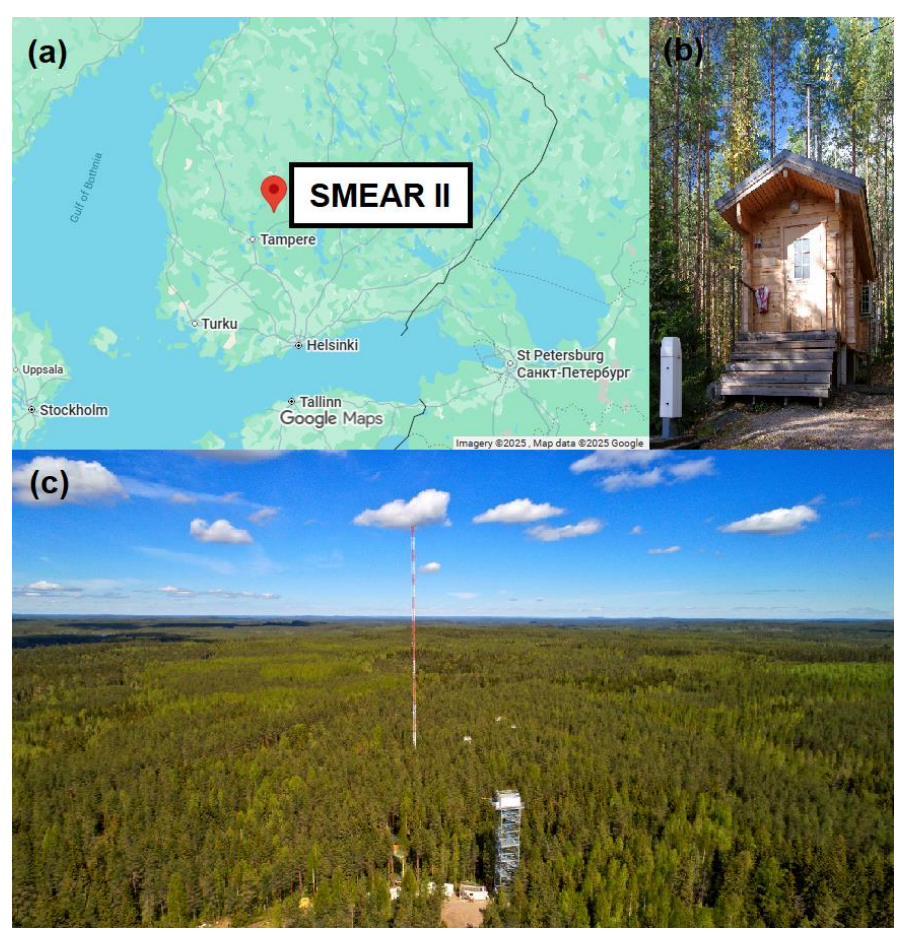


Figure 1: (a) The location of SMEAR II (Map data ©2025 Google), (b) cottage for aerosol instrumentation (photo by Juho Aalto), and (c) a photo of the surrounding region around SMEAR II (photo by Juho Aalto and Matti Loponen).

2.2 Weighing-based mass measurements with cascade impactor

PM measurements with gravimetric cascade impactor started in late 1990s at SMEAR II. The impactor has an unheated TSP inlet with stainless-steel tube, placed at 5 m height above the ground. The cascade impactor has three stages with impactor cut points at 10 μ m (PM₁₀), 2.5 μ m (PM_{2.5}) and 1 μ m (PM₁) (Dekati PM10 impactor) (Berner and Luerzer, 1980). The sample air flow rate during collection is 30 l min⁻¹. Collection substrates are 25 mm polycarbonate membranes (Nuclepore 800 203) without holes. At the last stage there is a 47 mm Teflon filter with 2 μ m pore size (R2P J047) from Pall Corporation. To prevent the bouncing back of the particles from the collection substrates, the membranes are greased with Apiezon L vacuum grease diluted in toluene. The impactor samples are collected for two to three days, before the filters are taken to a clean laboratory room, where they are dried in

174 laminar flow hood for at least two hours before weighting to get the mass distribution. The 175 samples are stored in a freezer for occasional further analyses. 176 177 2.3 Online mass measurements with SHARP 178 The Synchronized Hybrid Ambient Real-time Particulate Monitor (SHARP, Thermo 179 Scientific, Model 5030) is a real-time particulate monitor measuring at 1 s time resolution 180 (Goohs et al., 2009). SHARP combines light scattering photometry and β -ray attenuation for 181 continuous PM₁₀ measurement. In SHARP the light scattering signal (nephelometer) is 182 automatically calibrated against the beta attenuation mass sensor. The sample line inlet is placed on the roof of the cottage at 6 m height above the ground level and its flow rate is 16.7 183 1 min⁻¹. The sample line is heated to reduce the humidity of the sample air. The temperature 184 was fixed to 45 °C until August 2016 and to 35 °C after that. The sensitivity of the instrument 185 was calibrated regularly with a specific foil. Sampling with SHARP at SMEAR II started in 186 2012. 187 2.4 Aerosol mass derived from the particle size distribution 188 The aerosol mass concentration for different size classes PM₁₀, PM_{2.5} and PM₁ can also be 189 190 estimated by combining the number size distributions measured with Differential Mobility 191 Particle Sizer (DMPS) and Aerodynamic Particle Sizer (APS) and calculating the mass by 192 assuming that the particles are spherical and have a constant density. The instrument set-ups 193 for DMPS and APS are described in detail by Aalto et al. (2001). Briefly, the twin-DMPS 194 consists of a long and a short Vienna type Differential Mobility Analyzers (DMA) and two 195 condensation particle counters (CPC; TSI 3025 and TSI 3775). The DMPS inlet is placed on 196 the roof of the cottage at 8 m height and APS inlet at 5 m above ground level. The DMPS and APS systems provide aerosol number size distribution with a 10 min time resolution. The 197 APS inlet line is heated to 35 °C, similarly as the SHARP inlet line. In the DMPS system, the 198 sheath flow is dried with a silica diffusion dryer. The relative humidity of the sheath flow was 199 200 kept below 40 %. The calibrations of both instruments are checked regularly using 201 polystylene latex spheres. 202 203 At SMEAR II, the DMPS measures the aerosol number size distribution in the electrical mobility equivalent diameter range of 3–1000 nm (Aalto et al., 2001). The APS (TSI 3320) 204 205 measures the aerodynamic particle size distribution of particles with aerodynamic diameter

within the range of 0.5–20 µm (Peters et al., 2006). To have comparable particle size

207 distributions, we converted the aerodynamic diameter (d_a) of the APS to mobility equivalent

208 diameter ($d_{\rm m}$):

209

$$210 d_{\rm m} = \sqrt{\frac{\rho_0}{\rho_{\rm p}}} d_{\rm a}, (1)$$

211

- where ρ_p is the density of the particle and ρ_0 is the unit density of the particle (1 g cm⁻³). The
- 213 density of the particles is assumed to be 1.5 g cm⁻³ (Saarikoski et al., 2005; Kannosto et al.,
- 214 2008), but we additionally calculated the mass concentrations using 1.1 and 2.0 g cm⁻³
- 215 densities, which are the minimum and maximum densities of accumulation mode sized
- 216 particles at SMEAR II (Kannosto et al. 2008) to understand the importance of constant
- 217 density assumption to the particle mass. The mass of the particles measured with
- 218 DMPS+APS is calculated as:

219

220
$$m = \frac{1}{6}\rho_{\rm p}\pi d_{\rm m}^3$$
. (2)

221

- The mass concentrations (PM₁, PM_{2.5} and PM₁₀) were then calculated by integrating over the
- 223 corresponding size range:

224

225
$$PM_i = \int_{0 \mu m}^{0.6 \mu m} N_{DMPS} \cdot m_{DMPS} dd_m + \int_{0.6 \mu m}^{i \mu m} N_{APS} \cdot m_{APS} dd_m$$
 (3)

226

- 227 In practice, we utilized DMPS data from 0.003 to 0.6 µm and APS size distribution from 0.6
- 228 μ m to 1 μ m, 2.5 μ m or 10 μ m, depending on the mass fraction in question. Typical size
- 229 distributions for different seasons are presented in Fig. 2.

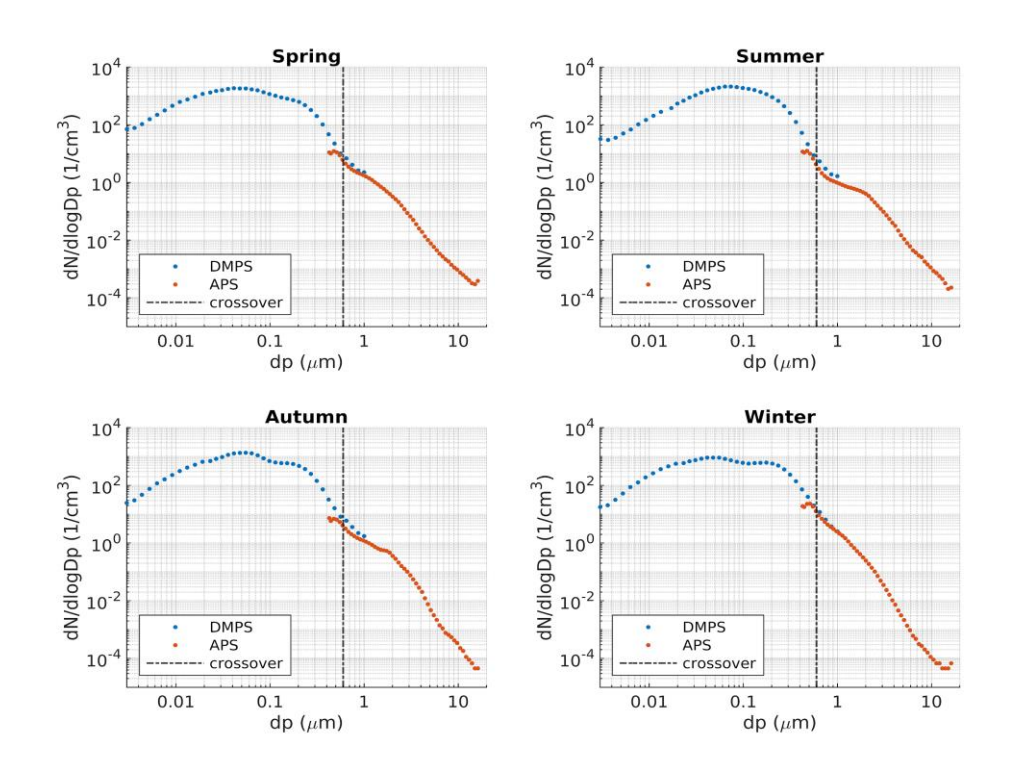


Figure 2: Seasonal median number size distributions for 2005–2020 at SMEAR II measured with a combination of DMPS and APS with a constant density assumption. The dash-dotted line indicates the crossover size between the instrument data to determine integrated mass concentrations.

2.5 Ancillary data

 SO_2 and NO_x were measured at 16.8 m height above ground level at SMEAR II with gas analyzers by Thermo Fisher Scientific Inc., USA. SO_2 was measured with pulsed fluorescence technique, using model TEI 43CTL until September 2010 and model TEI 43i-TLE after that. NO_x concentration was measured with TEI 42CTL (molybdenum converter) until February 2007, then with TEI 42CTL (photolytic converter) until April 2011, and after that with TEI 42iTL (photolytic converter).

Monoterpene concentration was measured with quarupole Proton Transfer Reaction Mass Spectrometer (PTR-MS; Ionicon, Austria). We used concentration measured at 16.8 m height. The measurement setup is described in Taipale et al. (2008) and Rantala et al. (2014).

Equivalent black carbon (eBC) concentration was derived by filter-based optical instruments:

Aethalometer (Magee Scientific, model AE31) in years 2006–2017 and Multi-Angle

251 Absorption Photometer (MAAP; Thermo Fisher Scientific, model 5012) in years 2013–2020. The correction procedure for AE31 data at SMEAR II as well as the measurement setup of 252 253 AE31 and MAAP are described in detail in Luoma et al. (2021). The AE31 data were 254 corrected by using a correction algorithm described in Virkkula et al. (2007) and using a 255 multiple scattering correction factor of 3.14, which was derived by comparing the AE31 to 256 MAAP. To derive the eBC concentration from the measured absorption coefficient, a mass absorption cross section values of 6.6 and 4.78 m² g⁻¹ were used for MAAP at wavelength 257 637 nm and AE31 at wavelength 880 nm, respectively. 258 259 Air mass origins were calculated using Hybrid Single-Particle Lagrangian Integrated 260 Trajectory model (HYSPLIT) (Stein et al., 2015). The arrival height of the trajectories was 261 262 100 m, and they were calculated 96 h backwards in 1 h resolution. The trajectories were 263 divided into three sectors as described in Räty et al. (2023). Clean sector (Fig. S5e) represents 264 area with minor anthropogenic contribution, while European and Eastern sectors represent more pollutant air mass source areas (Niemi et al., 2009; Riuttanen et al., 2013). Trajectory 265 266 was classified into certain sector when it spent at least 90 % of the time in that sector, 267 otherwise it was classified as mixed. 268 269 2.6 Correlations, bivariate fitting and long-term trend estimation 270 The Pearson's correlation coefficients between the mass concentrations from different 271 instruments were calculated in Matlab, along with bivariate fitting (Cantrell, 2008). Before 272 the analysis, we removed clear outliers that were further than 6 scaled median absolute 273 deviations (MAD) away from the median using the Matlab built-in function isoutlier. The procedure was done for the whole dataset at once, i.e. without regarding for instance seasonal 274 275 dynamics, but separately for each instrument and PM size. The limit was determined using visual inspection. About 1.5 % of the data were removed. When comparing DMPS+APS and 276 277 SHARP with the impactor data, we calculated 2–3 days' cumulative aerosol mass 278 concentration to make DMPS+APS and SHARP measurements comparable to the impactor 279 data time resolution. 280 281 The statistical significance of long-term trends in linear scale were calculated using the 282 mannkendall function for Matlab (v1.1.0, 10.5281/zenodo.4495589). We applied the seasonal 283 3PW method, which utilizes three pre-whitening methods for the trend estimation (Hirsch et

al., 1982). Pre-whitening methods by Kulkarni and von Stroch (1995) and Yue et al. (2002) remove lag-1 autocorrelation and autocorrelation on detrended data, enabling to determine the statistical significance of Mann-Kendall test reliably; of these the one with higher value is reported. Variance-corrected trend-free pre-whitening method by Wang et al. (2015) is used for calculation of Sen's slope, which leads to more accurate trend analysis (Collaud Coen et al., 2020).

3 Results and discussion

3.1 Comparison between the mass measurement methods

Here, we present the comparison between the different aerosol mass measurement techniques at SMEAR II (Fig. 3 and S1a). We found that the data from the different mass measurement techniques correlate well, with the correlation coefficients R > 0.8 for all the measurements except between SHARP and impactor for which R = 0.74 (Table 1). Thereby, the correlation was lower between the two direct mass measurements, SHARP and impactor, than between DMPS+APS derived and impactor or SHARP measurements, even though with the DMPS+APS method we had to assume constant density and spherical shape of the particles in the mass concentration calculations. In reality, the particle composition, density, and shape vary between different particles (Kannosto et al., 2008; Heikkinen et al., 2020), which could potentially lead to the higher uncertainty in the indirect DMPS+APS mass calculations.

Table 1: Correlation coefficients between different PM measurement techniques. Correlation coefficient between SHARP and DMPS+APS in PM₁₀ was 0.84. In all cases P-value << 0.05.

Method	Impactor, PM ₁₀	Impactor, PM _{2.5}	Impactor, PM ₁
DMPS+APS	0.84	0.86	0.88
SHARP	0.74	-	-

To estimate the impact of selected density in DMPS+APS method, we calculated the average mass concentrations using 1.1 and 2.0 g cm⁻³ as lower and upper estimates of the particle densities (Kannosto et al., 2008). The average PM mass concentrations for 2005–2020 are presented in Table S1. The average mass concentrations calculated with 1.1 g cm⁻³ particle density were 7–12 % smaller compared to the mass obtained with 1.5 g cm⁻³ density for

 PM_{10} , 12–20 % for $PM_{2.5}$, and 20–25 % for PM_1 . Correspondingly, with 2.0 g cm⁻³ particle density, the calculated mass concentrations were 14–17 % larger for PM_{10} , 19–27 % for $PM_{2.5}$, and 29–30 % for PM_1 .



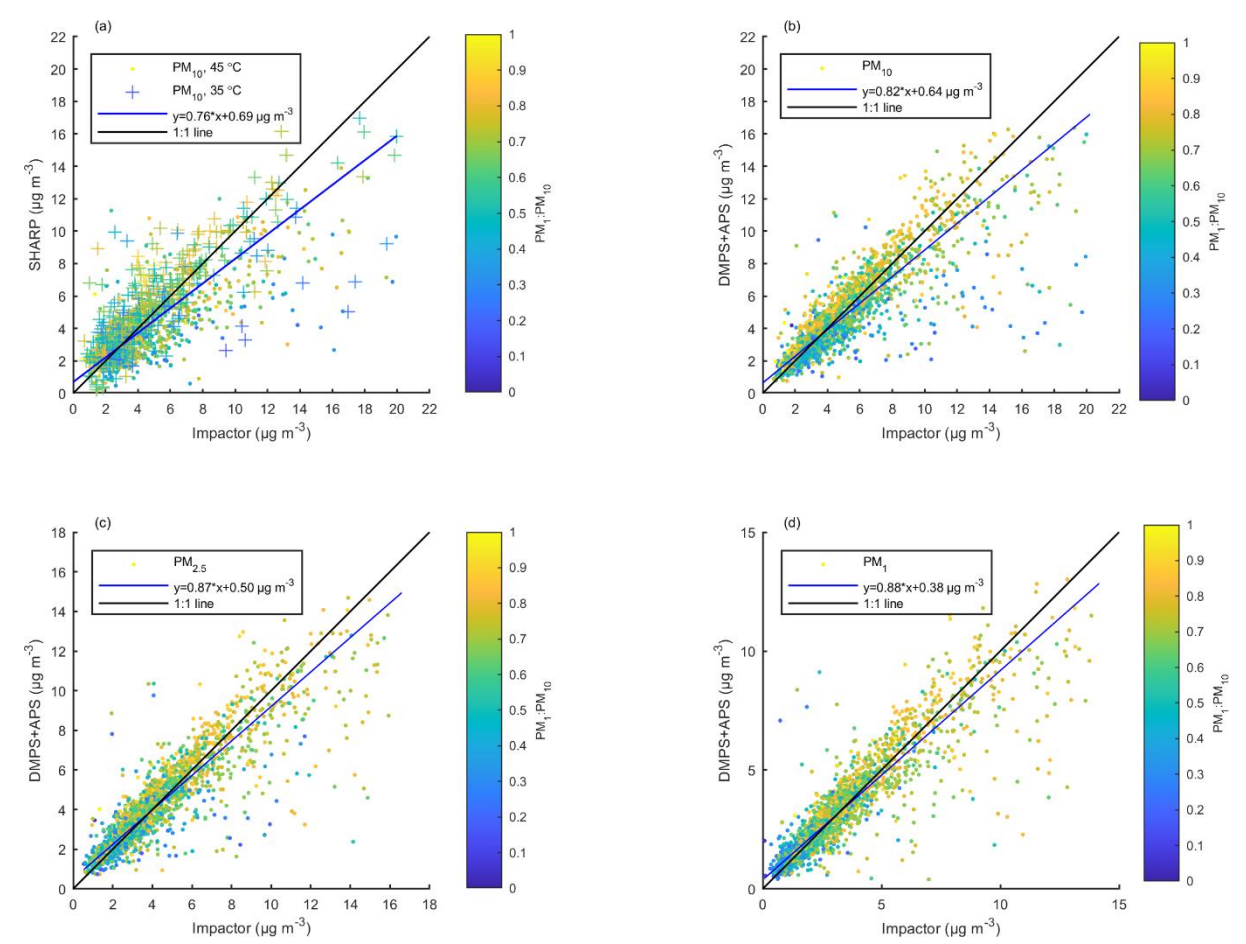


Figure 3: Correlation between the different mass measuring methods against impactor measurements a) PM_{10} from SHARP, b) PM_{10} from DMPS+APS, c) $PM_{2.5}$ from DMPS+APS, and d) PM_1 from DMPS+APS. Bivariate fit to the data is represented with a blue line and 1:1 line is black. Color is PM_1 to PM_{10} ratio from impactor measurements and in (a) markers differentiate the inlet heating temperature of SHARP (circle = 45 °C and plus sign = 35 °C). The data are averaged based on the impactor time resolution (2–3 days).

Comparing Fig. 3 and Fig. S1a, it seems that the data points between SHARP and DMPS+APS are positioned more distinctly on the 1:1 line whereas the impactor data are scattered more towards higher concentrations in all size classes. After the inlet heating temperature reduction in SHARP from 45 to 35 °C, the PM₁₀ values measured by SHARP were more comparable to those measured by impactor, except for the lowest and highest PM₁₀ concentrations (Fig. S2a–b). When comparing to DMPS+APS data (Fig. S2c–d),

330 SHARP also showed slightly lower PM₁₀ concentrations when the inlet was heated to 45 °C, and mostly similar concentrations (within standard deviation) when inlet was heated to 35 °C. 331 Again, with the lowest concentrations, SHARP showed higher variability in the measured 332 333 PM₁₀ concentrations. When excluding the lowest mass concentrations (approximately below 1.5 µg m⁻³), with 45 °C inlet heating SHARP to impactor ratio was 0.65 and SHARP to 334 DMPS+APS ratio 0.85. With 35 °C inlet heating, the ratios were 0.91 and 1.0, respectively. 335 336 This indicates that the higher inlet heating temperature might have led to 15–25 % losses of 337 semi-volatile compounds from the sample air of SHARP. 338 339 Color in Fig. 3 and S1a is PM_1 to PM_{10} ratio from impactor measurements. In general, the 340 correlations between instruments were rather independent of the fractions of different particle 341 sizes, but in PM₁₀ correlation with impactor (Fig. 3a–b), the scattered data points have lower PM₁ to PM₁₀ ratio. This implies that the impactor PM₁₀ measurements were likely 342 343 overestimated in these cases since in PM₁ and PM_{2.5}, as well as in the DMPS+APS 344 correlation with SHARP, PM₁ to PM₁₀ ratio from impactor data seem to be more evenly 345 distributed (Fig. 3c-d and S1a). We additionally plotted correlation between monthly median 346 concentration of PM₁ and PM_{2.5} as well as PM_{2.5} and PM₁₀ from DMPS+APS and impactor 347 measurements (Fig. S1b). The figure shows that while the data from DMPS+APS is rather 348 well aligned with 1:1 line, the PM₁₀ against PM_{2.5} from impactor data has more scattered data 349 points, further implying that the impactor data might be overestimated. 350 351 In Waldén et al. (2010) different PM analyzers were tested for air quality monitoring in 352 Helsinki. They reported that the two tested SHARP instruments passed the equivalence tests 353 for PM₁₀ monitoring while for the PM_{2.5} measurements a calibration correction factor had to 354 be applied. In their instruments, inlet lines were heated to 35 °C. They also reported that 355 while Dekati PM10 impactor was overall indicative measurement method for PM2.5 (other sizes were not measured), it overestimated the concentrations compared to the reference 356 methods. For the impactor, they used 24 h sampling period with 30 l min⁻¹ flow rate. 357 358 359 The measurement methods used in this study differ considerably from each other, and hence they are subject to different kinds of issues in PM monitoring. The impactor data, for 360 example, is sensitive to any disturbances related to the weighing of the filters or evaporation 361 of semi-volatile material from the filters during the long sampling time. The impactor is, 362

however, the only purely weighing-based mass measurement at SMEAR II. Thus, in the next section, we compare all the other methods against the impactor data. 3.2 PM concentrations, seasonal variation, and emission events We explore the time series of PM concentrations to observe overall concentration levels, seasonal differences, and specific emission events (Fig. 4 and S2). Mean values from 1991– 2002 reported by Laakso et al. (2003) are also included in the figures to compare the results with the earlier values from SMEAR II. To enable the comparison with the values by Laakso et al. (2003), we present mean and median concentrations of shorter, approximately five-year periods (2005–2010, 2011–2015, and 2016–2020) in Table 2.

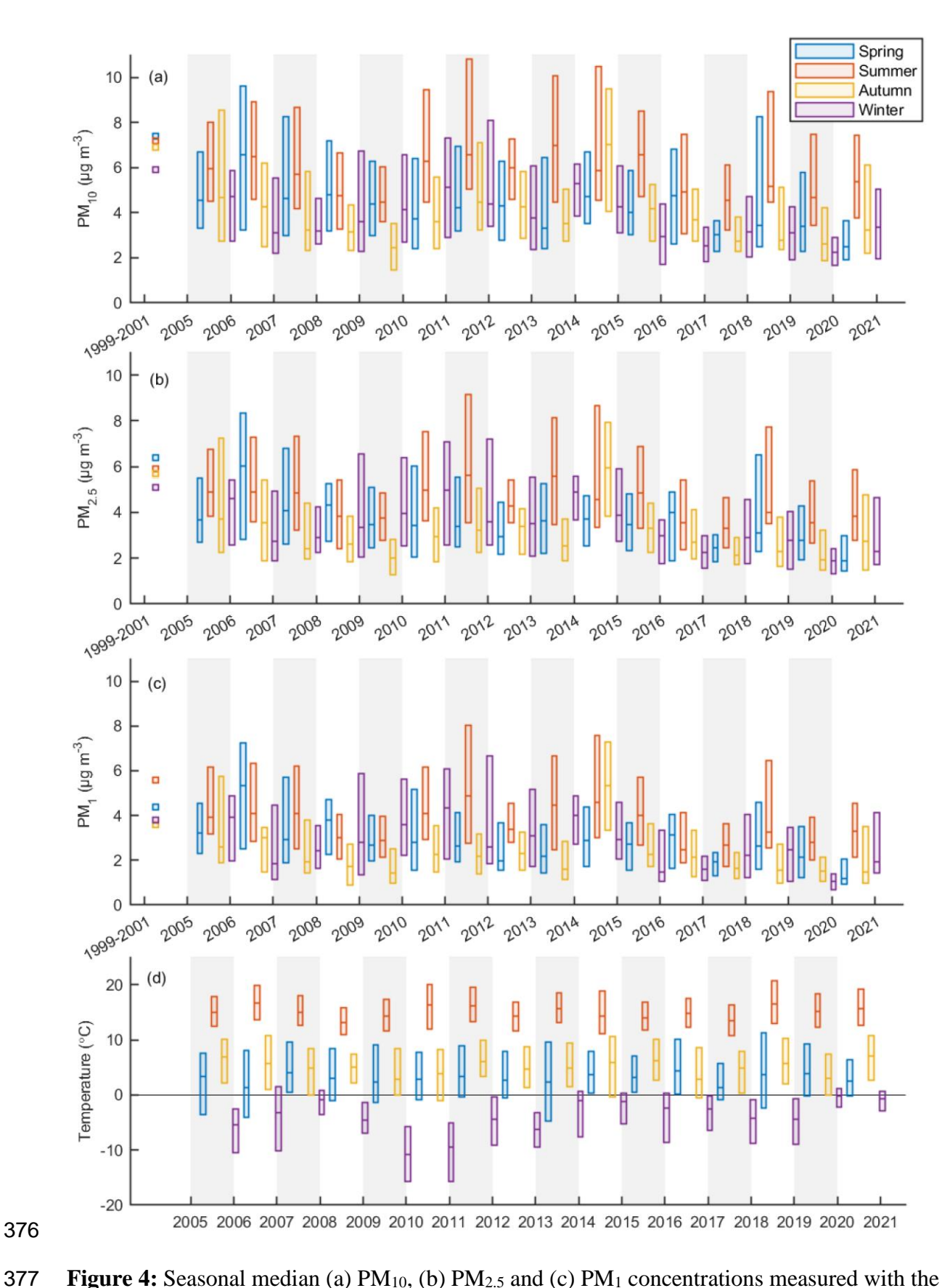


Figure 4: Seasonal median (a) PM₁₀, (b) PM_{2.5} and (c) PM₁ concentrations measured with the impactor as well as (d) temperature and their 25 and 75 quartile ranges at SMEAR II. The

tick marks on the x-axis are in the beginning of a year. Mean values for 1991–2002 are from Laakso et al. (2003).

Table 2: Average (mean / median) PM concentrations measured at SMEAR II. Values (mean) for 1999–2001 are from Laakso et al. (2003) and other values from this work. First number in each cell is the mean for the indicated period and following numbers are seasonal means. Unit is $\mu g \ m^{-3}$.

	1999–2001	2005–2010	2011–2015	2016–2020	2005–2020
PM ₁₀ , impactor -Spring -Summer -Autumn -Winter	6.9 7.4 7.2 6.9 5.9	5.4 / 4.4 5.9 / 4.7 6.4 / 5.6 4.5 / 3.4 4.7 / 3.9	5.8 / 4.8 5.3 / 4.2 7.4 / 6.4 5.4 / 4.4 5.0 / 4.4	4.4 / 3.4 4.4 / 3.3 5.8 / 5.5 4.1 / 3.0 3.3 / 2.8	4.5 / 4.2 4.2 / 4.1 5.5 / 5.6 4.3 / 3.5 3.9 / 3.6
PM ₁₀ , SHARP -Spring -Summer -Autumn -Winter	-	-	4.2 / 3.6 4.0 / 3.5 4.9 / 4.4 3.8 / 3.1 4.1 / 3.3	4.7 / 4.0 4.4 / 3.6 6.0 / 5.5 4.7 / 3.8 3.8 / 3.3	5.2 / 3.8 5.2 / 3.6 6.5 / 5.1 4.7 / 3.7 4.4 / 3.3
PM ₁₀ , DMPS+APS -Spring -Summer -Autumn -Winter	-	5.5 / 4.8 5.8 / 4.9 6.2 / 5.9 4.8 / 3.9 5.5 / 4.7	4.8 / 4.0 4.4 / 3.9 5.9 / 5.0 4.2 / 3.3 4.7 / 3.9	4.2 / 3.4 4.1 / 3.5 5.5 / 4.9 3.8 / 2.8 3.5 / 2.9	4.9 / 4.1 4.8 / 4.1 5.9 / 5.3 4.3 / 3.4 4.7 / 3.9
PM _{2.5} , impactor -Spring -Summer -Autumn -Winter	5.8 6.4 5.9 5.7 5.1	4.6 / 3.7 5.0 / 4.1 5.2 / 4.6 3.6 / 2.7 4.4 / 3.5	4.7 / 3.8 4.2 / 3.5 5.9 / 5.0 4.2 / 3.4 4.5 / 3.8	3.5 / 2.8 3.4 / 2.6 4.5 / 3.7 3.3 / 2.3 2.9 / 2.4	4.3 / 3.4 4.2 / 3.3 5.2 / 4.4 3.7 / 2.8 4.0 / 3.2
PM _{2.5} , DMPS+APS -Spring -Summer -Autumn -Winter	-	4.7 / 4.0 4.8 / 4.2 5.1 /4.8 3.9 / 3.2 5.1 / 4.3	4.1 / 3.4 3.7 / 3.2 4.9 / 4.2 3.5 / 2.7 4.3 / 3.6	3.6 / 3.0 3.4 / 2.9 4.6 / 4.2 3.3 / 2.4 3.3 / 2.8	4.2 / 3.6 4.1 / 3.4 4.9 / 4.5 3.6 / 2.8 4.3 / 3.6
PM ₁ , impactor -Spring -Summer -Autumn -Winter PM ₁ ,	4.3 4.4 5.6 3.6 3.8	3.8 / 3.0 4.2 / 3.4 4.4 / 3.7 2.8 / 2.1 3.7 / 2.8	3.8 / 2.9 3.3 / 2.7 4.9 / 4.0 3.3 / 2.3 3.7 / 3.0	2.7 / 2.1 2.6 / 2.0 3.5 / 3.0 2.4 / 1.6 2.3 / 1.7	3.4 / 2.7 3.4 / 2.7 4.2 / 3.5 2.8 / 2.0 3.3 / 2.5

DMPS+APS	-	3.8 / 3.3	3.3 / 2.6	3.0 / 2.4	3.4 / 2.8
-Spring		3.9 / 3.3	2.9 / 2.5	2.8 / 2.3	3.3 / 2.6
-Summer		4.2 / 3.9	4.1 / 3.6	3.8 / 3.3	4.0 / 3.6
-Autumn		3.0 / 2.3	2.7 / 1.9	2.6 / 1.8	2.8 / 2.1
-Winter		4.3 / 3.4	3.5 / 2.8	2.7 / 2.0	3.5 / 2.8
	I				

The PM concentrations in all size classes are typically highest in summer and lowest in autumn (Table 2). In summertime, the surrounding boreal forest is a large source of organic compounds (Fig. S4c), which contribute to the aerosol load as shown already in several studies (e.g. Heikkinen et al., 2020; 2021; Yli-Juuti et al., 2021). Due to the temperature dependent activity of the forest, warm spells and heatwaves increase the VOC emissions, such as in 2018 (Fig. S4c; Neefjes et al., 2022), which is also evident in the PM data in all size classes (Fig. 4). Furthermore, pollen and other biological particles contribute especially to coarse mode particle mass at SMEAR II from late spring to early autumn (Manninen et al., 2014).

Although PM mass concentrations are generally decreasing (Fig. 4), certain events associated with higher PM levels, such as wildfires and volcanic eruptions, can be detected. In 2006 springtime as well as in 2006 and 2010 summer forest fires in eastern Europe increased the measured PM concentrations at SMEAR II (Fig. 4) as seen also in Anttila et al. (2008) and Leino et al. (2014). The growing seasons of 2006 and 2011 were exceptionally warm at SMEAR II based on the analysis spanning years 1996–2017 (Pysarenko et al., 2022), which is also visible in PM concentrations (Fig. 4), but the relatively high PM concentrations in spring 2010 and 2011 can also be caused by the plume of ash and SO₂ from the erupted Eyjafjallajökull (Thomas et al., 2011; Gudmundsson et al., 2012; Flanner et al., 2014) and Grímsvötn (Cooke et al., 2011; Tesche et al., 2012) volcanoes in Iceland. The considerably higher PM concentrations in autumn 2014 were affected by eruptions of Bardarbunga (Gislason et al., 2015) and Holuhraun (Ilyinskaya et al., 2017) volcanoes in Iceland, which Heikkinen et al. (2020) also noticed in the sulfate aerosol and SO₂ concentrations.

During the coldest winters 2009–2010 and 2010–2011, the measured PM concentrations were high (Fig. 4 and S2). These years were also associated with high concentrations of SO₂, NO_x, and eBC (Fig. S4). Residential heating is known to be a source of particulate emissions as wood is burned for heating (Spindler et al., 2004; Viana et al., 2008; Barmpadimos et al., 2011). However, the coldest winter temperatures are typically measured in Finland when air

416 is transported from the eastern continental areas (Sui et al., 2020). These, and particularly 417 southeastern, areas are also a source of atmospheric pollutants (Niemi et al., 2009; Riuttanen et al., 2013). Hence, rather than being local, pollutants can also be advected to Finland. Air 418 419 mass source area analysis shows that winters with higher fraction of easterly air masses (Fig. 420 S5) were colder and had also higher PM levels, although we acknowledge that this analysis 421 does not reveal the actual source of the measured PM. Further, boundary layer height 422 dynamics affect the measured concentrations, because shallow boundary layer heights during 423 cold winter days can concentrate the anthropogenic pollutants close to the surface (Stull, 424 1988; Sinclair et al., 2022). 425 426 Overall, the air quality at SMEAR II was very good during our measurement period from 427 2005 to 2020. The average concentrations measured by impactor were 4.5, 4.3, and 3.4 µg m⁻¹ ³ for PM₁₀, PM_{2.5}, and PM₁, which are in line with PM_{2.5} concentrations measured in 2002 428 429 and 2010 at background stations in Sweden and Norway (average PM_{2.5} ranging from 4.3 to 9.9 µg m⁻³ (Cusack et al., 2012)) and generally lower than at other background stations in 430 Europe (average PM_{2.5} ranging from 5.5 to 26.2 µg m⁻³ (Cusack et al., 2012)). 431 432 433 3.3 Long-term trends 434 The measured PM concentrations show a declining trend during the measurement period 435 from 2005 to 2020 (Fig. 4). Compared to the values reported by Laakso et al. (2003) for 1999–2001 (6.9, 5.8, and 4.3 μ g m⁻³ for PM₁₀, PM_{2.5}, and PM₁, respectively), the values in 436 2016–2020 are almost 40 % lower in all size classes (Table 2). 437 438 While the overall PM concentrations are decreasing, the different mass measurement methods 439 440 gave slightly inconsistent results: DMPS+APS method shows constant decline in PM 441 concentrations, whereas the impactor data shows slight increase in all PM sizes for 2011– 442 2015 period for all seasons but spring (Table 2). The clearest difference between the impactor 443 and DMPS+APS data seems to be the steadier decline in autumn concentrations in 444 DMPS+APS data (Fig. 4 and Fig. S2b-c). Hence, despite the discrepancies the methods give 445 generally comparable results. 446 447 SHARP data shows increased PM₁₀ concentration between 2011–2015 and 2016–2020 for all

other seasons except for winter, but this is likely explained by the decreased inlet heating

temperature, changed between the two periods (Fig. S3). Hence, no further conclusions of the trend in SHARP data can be drawn, even though generally the concentrations measured by SHARP follow the concentrations measured by DMPS+APS method (Fig. S2a-b).

Long-term trends are shown seasonally for each size class PM₁₀, PM_{2.5}, and PM₁ using impactor (Fig. 5, S6, and S7), and DMPS+ APS data (Fig. S8–S10). Calculated seasonal and annual trends are presented in Table 3. On seasonal scale, decreasing trends, ranging from -0.007 to -0.066 μg m⁻³ y⁻¹, are observed in each measured size class, while on annual scale, the trends vary between -0.021 and -0.036 μg m⁻³ y⁻¹. In general, the largest decreases in all size classes are observed in winter, whereas the decrease is the lowest in autumn. For the impactor method, the decline is statistically significant at 95 % level in spring and winter, but not in summer and autumn. However, when calculating the trends from DMPS+APS data using 6-hour averages, the Mann-Kendall test revealed a statistically significant decrease in all size classes and seasons (Fig. S8–S10).

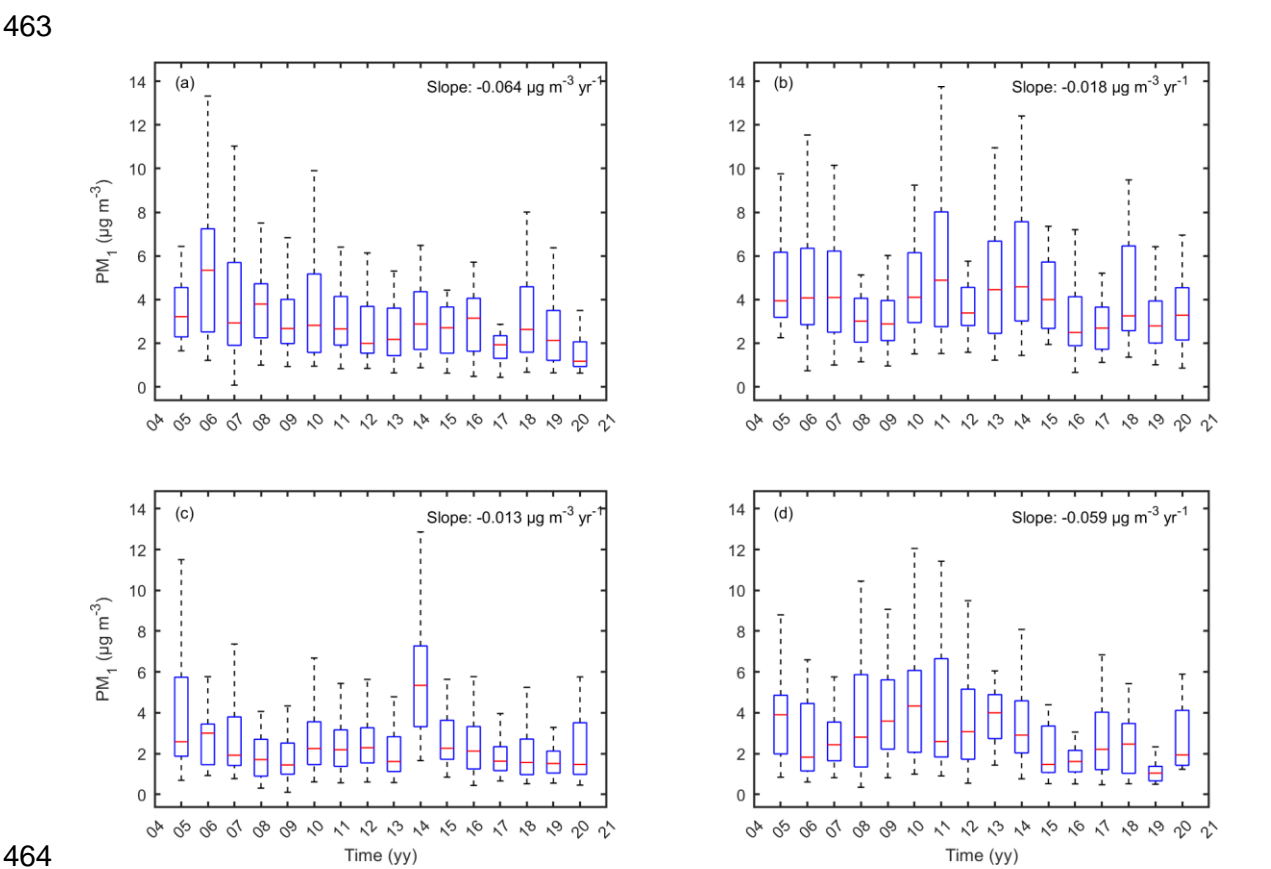


Figure 5: PM₁ concentration with the impactor method in (a) spring, (b) summer, (c) autumn, and (d) winter. Red horizontal line represents the median, the distance between the box edges shows the interquartile range, and whiskers extend to 1.5 times the interquartile range.

Outliers are not shown. Slope represents trend calculated using Sen's slope and statistical significance is calculated using Mann-Kendall test. The trends were statistically significant in spring and winter, but not in summer and autumn.

The seasonal differences in PM trends follow the trends observed also in SO₂ and NO_x concentrations (Fig. S11 and S12), as well as in eBC (Fig. S4d-e). Further, Luoma et al. (2019) showed that the relative decline of light absorbing aerosol is faster than the light scattering aerosol at SMEAR II, and that the decline was strongest in spring and winter. Hence, the results imply that the decrease in anthropogenic pollutants drive the decrease in PM, which has been seen also elsewhere (e.g. Yttri et al., 2021). On the other hand, the lower summer and autumn time decline can also be explained by the high fraction (more than 50 %) of OA from the surrounding boreal forest in the PM mass concentration at SMEAR II (Heikkinen et al., 2020). Further, in Li et al. (2023) the concentrations of organic precursors have even been shown to have an increasing trend at SMEAR II.

Table 3: Annual and seasonal trends in 2005–2020 PM concentrations at SMEAR II. Results from the DMPS+APS method are calculated from 6 h averages while impactor data has original time resolution (averaged over 2–3 days). Results, which are not statistically significant in 95 % level, are marked with *. Unit is μg m⁻³ y⁻¹ except the second number in annual trends which is % y⁻¹.

	Method	Spring	Summer	Autumn	Winter	Annual
PM ₁₀	Impactor	-0.053	-0.018*	-0.017*	-0.056	-0.035 / -0.59
	DMPS+APS	-0.038	-0.012	-0.016	-0.066	-0.032 / -0.56
PM _{2.5}	Impactor	-0.059	-0.020*	-0.012*	-0.057	-0.034 / -0.70
	DMPS+APS	-0.034	-0.013	-0.009	-0.061	-0.028 / -0.56
PM ₁	Impactor	-0.064	-0.018*	-0.013*	-0.059	-0.036 / -0.89
	DMPS+APS	-0.027	-0.013	-0.007	-0.042	-0.021 / -0.52

In winter, biogenic OA precursors have minima in their concentrations (Fig. S4c), as shown also in Heikkinen et al. (2020), and consequently the collected PM originates mostly from anthropogenic sources, such as traffic, industry, and different combustion processes (Forsberg et al., 2005; Anttila & Tuovinen, 2010) as is indicated by the winter maxima in eBC concentrations (Fig. S4d-e). Moreover, many gaseous pollutants, emitted from

494 anthropogenic processes and contributing to atmospheric chemistry or aerosol processes, such as SO₂ and NO_x, have maxima in their seasonal cycle in spring and winter (Fig. S4a-b; 495 496 Lyubovtseva et al., 2005; Anttila & Tuovinen, 2010; Riuttanen et al., 2013; Heikkinen et al., 497 2020), further affirming the contribution of anthropogenic pollution to the observed trends. 498 Additionally, Banerji et al. (2025) showed that at SMEAR II, light absorbing aerosol peak in 499 winter, being thus associated with e.g. black carbon from anthropogenic activities, while 500 aerosol scattering peaks in summer and winter, being thus likely associated with organic aerosol in summer and sulfates in winter. They also found an increasing trend in single 501 502 scattering albedo, indicating that the relative proportion of light absorbing aerosol decrease. Luoma et al. (2019), in turn, reported decreased light scattering and absorption with a 503 504 simultaneous increase in light backscattering fraction and scattering Ångström exponent at SMEAR II, indicating reduction in large particle concentration. 505 506 507 The seasonal difference in PM sources is visible also in the ratios between PM₁ to PM_{2.5} and 508 PM_{2.5} to PM₁₀ plotted against temperature bins (Fig. 6) as well as in monthly PM₁ to PM₁₀ 509 ratio (Fig. S13). The fraction of smaller particles increases in cold and warm temperatures (Fig. 6), which could be attributed to anthropogenic pollution during winters and secondary 510 511 aerosol formation in summer, which is also visible in aerosol PM₁ to PM₁₀ aerosol light scattering coefficient (Luoma et al., 2019). In winters, nearly 80 % of PM₁₀ consists actually 512 513 of PM_1 (Fig. S13). 514 515 The PM₁ to PM_{2.5} and PM_{2.5} to PM₁₀ ratios exhibit small, but statistically significant at the 95 % confidence level, negative trends (Fig. S14). The decline is particularly attributed to the 516 517 decline in PM₁ concentration due to decreasing anthropogenic precursor concentrations since 518 the it is larger in PM₁ to PM_{2.5} ratio. Also, the annual relative trends from the impactor data 519 are largest for PM₁ (Table 3). Sweden at two regional background sites, the PM_{2.5} to PM₁₀ ratios in 1999–2001were 0.77 and 0.8 (Forsberg et al., 2005), which is in line with the 520 measurements from SMEAR II. In 1999–2001 dataset, the PM_{2.5} to PM₁₀ ratio at SMEAR II 521 was 0.86 in winter and spring, and 0.82 in summer and autumn (Laakso et al., 2003) while in 522 523 2020, the ratios fell below 0.8 (Fig. S14) also highlighting the change in aerosol population at SMEAR II. 524 525

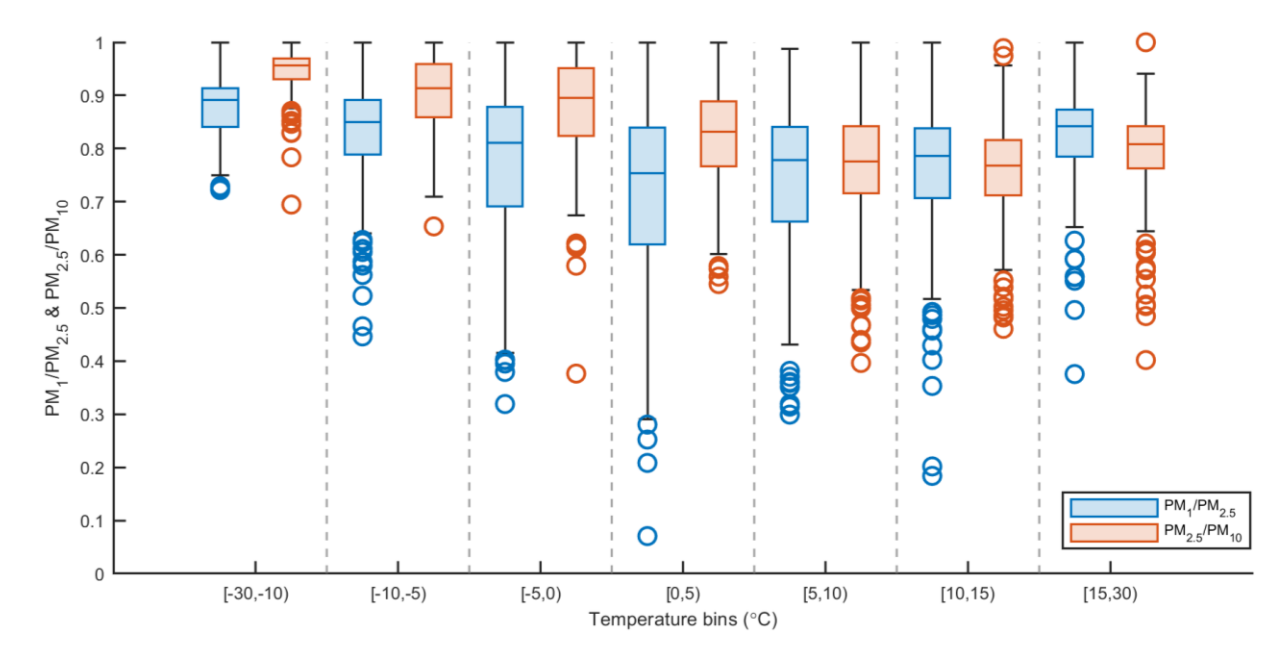


Figure 6: PM₁ to PM_{2.5} and PM_{2.5} to PM₁₀ ratios in different temperature bins using impactor data. Horizontal line represents the median, the distance between the box edges shows the interquartile range, whiskers extend to 1.5 times the interquartile range, and data points even further from the median are presented with circles.

Generally, the PM concentrations have been observed to decrease in Europe (Spindler et al., 2004; Barmpadimos et al., 2011; Keuken et al., 2012; Guerreiro et al., 2014). However, in Guerreiro et al. (2014) non-significant positive trends in PM₁₀ (2002–2011) and PM_{2.5} (2006–2011) were also observed at Finnish rural background sites. In Anttila & Tuovinen (2010) both increasing and decreasing trends were detected in a dataset from 1994 to 2007 from Finland, which they linked to different measurement environments (urban, suburban, and industrial). Table 4 lists trends observed at different measurement sites across Europe.

Table 4: Summary of PM trends in previous literature. Unit is μg m⁻³ y⁻¹ except in Anttila & Tuovinen (2010) where the unit of the first number is μg m⁻³ month⁻¹ and the second is % yr⁻¹. Note that the trends are calculated using different methods.

PM_{10}	$PM_{2.5}$	Time	Location	Author
-0.15 to -1.2		1991–2008	Switzerland,	Barmpadimos
			various sites	et al., (2011)
-0.4	-0.4	1998–2010	Europe, various	Barmpadimos
			sites	et al., (2012)

		-1.9	2002–2010	Spain, regional	Cusack et al.,
				background site	(2012)
		-1.8	2002–2010	Europe, regional	Cusack et al.,
				background sites	(2012)
3.4	2 to -1.95	2.30 to -0.62	2002–2011 (PM ₁₀)	Europe, rural	Guerreiro
			2006–2011 (PM _{2.5})	background sites	et al., (2014)
2.2	29 to -4.11	1.19 to -1.91	2006–2011	Europe, (sub)urban	Guerreiro
				background sites	et al., (2014)
		-0.008 to	From 2005–2008	Italy, Po Valley,	Bigi & Gher-
		-1.717	to 2015	various sites	mandi, (2016)
-0.1	13 to -2.83	-0.26 to -2.03	2004–2014	Spain, various sites	Pandolfi et al.,
					(2016)
(0.024 to		1994–2007	Finland, various	Anttila &
	-0.054			sites	Tuovinen,
/ -(0.3 to -2.8				(2010)

The trends measured at SMEAR II (Table 3) are similar than reported previously for Finland, but lower than the trends observed elsewhere in Europe (Table 4). One reason for this is likely the overall lower PM concentrations at SMEAR II compared to other locations as well as the longer timespan. Moreover, the trends in different studies have been calculated using different methods, such as Sen's slope (this study; Cusack et al., (2012); Guerreiro et al., (2014); Paldolfi et al., (2016)), and generalized least squares regression (Anttila & Tuovinen, 2010; Bigi & Ghermandi, (2016)), and also using different data preprocessing, which can further affect the trend estimates.

The connection between decreasing gaseous pollutant emissions and secondary aerosol concentrations has already been noted previously (Anttila & Tuovinen, 2010; Cusack et al., 2012; Kyrö et al., 2014; Pandolfi et al., 2016; Li et al., 2023) and decreasing PM trends in Europe have been connected to modernization of industry and heating systems as well as technology development of vehicles (Spindler et al., 2004; Barmpadimos et al., 2011; Keuken et al., 2012). Hence, the observed decrease in PM concentrations at SMEAR II is in line with previous studies and can be connected to the emission reductions driven by air quality legislation.

561 **4 Conclusions** 562 In this paper, different long-term aerosol mass concentration (PM₁₀, PM_{2.5}, PM₁) 563 measurement techniques were compared and reported for the years 2005-2020 from SMEAR 564 II, Finland. The direct mass concentration measurements with a cascade impactor and SHARP were compared with the mass concentrations calculated from the combined aerosol 565 number size distributions of DMPS and APS. The results obtained using different methods 566 are well comparable with the correlation coefficients of about 0.8. 567 568 569 The lower correlation values were connected to sampling methodologies: e.g., reducing the 570 inlet heating temperature of SHARP increased the correlation with the impactor. 571 Additionally, although impactor measurements are simple and purely based on weighing of 572 filters, the impactor data showed somewhat higher concentrations than the other two 573 methods, especially in the PM₁₀ size, which might stem from the difficulties related to 574 weighing masses down to micrograms. Any disturbances or deposited dust particles can lead to overestimated mass concentration, which might be the reason why impactor data showed 575 576 statistically insignificant trends in summer and autumn while DMPS+APS data with similar absolute values resulted in statistically significant decreasing trend in PM concentration. On 577 annual scale, both methods indicated statistically significant decreasing trends, which were 578 579 comparable with the trends observed elsewhere in Finland. 580 The measured masses were similar between all the methods, and hence we can conclude that 581 all methods were applicable for long-term PM monitoring. Yet, we acknowledge that the 582 583 comparison of PM concentrations measured with different techniques gives valuable information for data quality control purposes, as well as for validating the applicability of the 584 585 different methods. Therefore, we encourage conducting extensive comparisons with different 586 methods at each measurement site. 587 The PM concentrations at SMEAR II were generally low, mostly less than 5 µg m⁻³, which 588 clearly fell below the 20 µg m⁻³ limit by the EU air quality legislation. The highest PM 589 590 concentrations at SMEAR II were measured in summer, when organic compounds from the 591 surrounding boreal forest contribute to the measured PM mass. Peaks observed in the PM 592 data can be related to transported particles from regions with e.g., forest fires or on-going

593

volcanic eruptions.

594	
595	The measurements showed overall decreasing PM trends for all size classes and in all
596	seasons, although the decline was faster in PM_1 size class, which can be attributed to the
597	decrease in anthropogenic pollution due to legislation aiming for improved air quality.
598	Importantly, the trends were weakest in summer when natural emissions of VOCs from the
599	forest lead to the formation of OA. As these natural VOCs are projected to increase with
600	increasing temperature, it is possible that summertime OA concentrations keep increasing in
601	the future. Taken together with the declining anthropogenic emissions, the role of natural
602	aerosol particles could be anticipated to signify in the future. Overall, the results emphasize
603	the importance of the long-term measurements (Kulmala et al., 2023) for understanding
604	atmospheric aerosol mass concentrations and factors controlling them. This is a requirement
605	to quantify the relative roles of natural and anthropogenic sources to PM concentrations and
606	ultimately to their impacts on health and climate.
607	Data availability
608 609 610 611	Aerosol data used in this study are available through EBAS database operated by NILU: https://ebas-data.nilu.no/ (accessed 05 May 2025), BC data is available at SmartSMEAR database at https://smear.avaa.csc.fi/ (accessed 05 September 2025), and temperature and trace gas data are published by Aalto et al. (2023) at https://doi.org/10.23729/23dd00b2-
612 613	b9d7-467a-9cee-b4a122486039 (accessed: 05 May 2025). Air mass source area data is available upon request from the corresponding author.
614	Author contribution
615 616 617 618 619	The idea and design of the study were conceived by HMK, MK, and TP. IY, HMK, and KLu wrote the manuscript, and together with LA analyzed the data and provided the visualizations. LH, TN, KLe, EE, MK, and TP helped to interpret the results. IY, HMK, LA, PA, JA, JL, KLu, SB, and JK were also providing measurement data. All authors also contributed to reviewing and commenting on the manuscript.
620	Competing interests
621	MK is member of the editorial board of Aerosol Research.
622	Acknowledgements
623	The authors acknowledge the SMEAR II and INAR RI infrastructure as well as ACTRIS for
624	the data accessed from SmartSMEAR (https://smear.avaa.csc.fi/) and EBAS

- 625 (https://ebas.nilu.no) databases. We thank also thank SMEAR II personnel and PIs for the
- 626 long-term measurement data.

Financial support

627

- We acknowledge the following projects: ACCC Flagship funded by the Research Council of
- 629 Finland grant number 337549 (UH), Academy professorship funded by the Research Council
- of Finland (grant no. 302958), Research Council of Finland projects no. 1325656, 311932,
- 631 334792, 316114, 325647, 325681, 347782, "Quantifying carbon sink, CarbonSink+ and their
- 632 interaction with air quality" INAR project funded by Jane and Aatos Erkko Foundation,
- 633 "Gigacity" project funded by Wihuri foundation, European Research Council (ERC) project
- 634 ATM-GTP Contract No. 742206, European Union via Non-CO2 Forcers and their Climate,
- Weather, Air Quality and Health Impacts (FOCI) and Horizon 2020 research and innovation
- program under grant agreements No. 654109 and 739530 (ACTRIS).

637 References

643

648

- Aalto, J., Aalto, P., Keronen, P., Kolari, P., Rantala, P., Taipale, R., Kajos, M., Patokoski, J.,
- Rinne, J., Ruuskanen, T., Leskinen, M., Laakso, H., Levula, J., Pohja, T., Siivola, E.,
- Kulmala, M., and Ylivinkka, I.: SMEAR II Hyytiälä forest meteorology, greenhouse gases,
- air quality and soil, University of Helsinki, Institute for Atmospheric and Earth System
- Research, https://doi.org/10.23729/23dd00b2-b9d7-467a-9cee-b4a122486039, 2023.
- Aalto, P., Hämeri, K., Becker, E., Weber, R., Salm, J., Mäkelä, J. M., Hoell, C., O'Dowd, C.
- D., Hansson, H.-C., Väkevä, M., Koponen, I. K., Buzorius, G., and Kulmala, M.: Physical
- characterization of aerosol particles during nucleation events, Tellus B: Chem. and Phys.
- 647 Meteorol., 53, 344-358, DOI:10.1034/j.1600-0889.2001.d01-25.x, 2001.
- Anttila, P., Makkonen, U., Hellén, H., Kyllönen, K., Leppänen, S., Saari, H., and Hakola, H.:
- 650 Impact of the open biomass fires in spring and summer of 2006 on the chemical composition
- of background air in south-eastern Finland, Atmospheric Environment, 42, 6472–6486,
- 652 https://doi.org/10.1016/j.atmosenv.2008.04.020, 2008.
- Anttila, P. and Tuovinen J.-P.: Trends of primary and secondary pollutant concentrations

- in Finland in 1994–2007, Atmospheric Environment, 44, 30-41,
- 656 doi:10.1016/j.atmosenv.2009.09.041, 2010.

- Anttila, P.: Air Quality Trends in Finland, 1994–2018, Academic dissertation in physics,
- 659 Institute of Atmospheric and Earth System Research / Physics, Faculty of Science, University
- of Helsinki, Helsinki, Finland, Finnish Meteorological Institute Contributions No. 163,
- https://helda.helsinki.fi/bitstream/handle/10138/320460/thesis-Pia-
- 662 <u>Anttilaweb.pdf?sequence=1&isAllowed=y</u>, 2020.

663

- Banerji, S., Luoma, K., Ylivinkka, I., Ahonen, L., Kerminen, V.-M., and Petäjä, T.:
- Measurement Report: Optical properties of supermicron aerosol particles in a boreal
- environment, EGUsphere [preprint], https://doi.org/10.5194/egusphere-2025-1776, 2025.
- Barmpadimos, I., Hueglin, C., Keller, J., Henne, S., and Prévôt, A. S. H.: Influence of
- meteorology on PM10 trends and variability in Switzerland from 1991 to 2008, Atmos.
- 669 Chem. Phys., 11, 1813-1835, DOI:10.5194/acp-11-1813-2011, 2011.

670

- Barmpadimos, I., Hueglin, C., Keller, J., Henne, S., and Prévôt, A. S. H.: Influence of
- 672 meteorology on PM₁₀ trends and variability in Switzerland from 1991 to 2008, Atmos. Chem.
- 673 Phys., 11, 1813–1835, https://doi.org/10.5194/acp-11-1813-2011, 2011.

674

- Barmpadimos, I., Keller, J., Oderbolz, D., Hueglin, C., and Prévôt, A. S. H.: One decade of
- parallel fine (PM_{2.5}) and coarse (PM₁₀–PM_{2.5}) particulate matter measurements in Europe:
- 677 trends and variability, Atmos. Chem. Phys., 12, 3189–3203, https://doi.org/10.5194/acp-12-
- 678 3189-2012, 2012.

679

- Berner, A. and Luerzer, C: Mass size distributions of traffic aerosols at Vienna, J. Phys.
- 681 Chem., 84, 2079-2083, DOI:10.1021/j100453a016, 1980.

682

- Bigi, A. and Ghermandi, G.: Trends and variability of atmospheric PM_{2.5} and PM₁₀–
- 684 2.5 concentration in the Po Valley, Italy, Atmos. Chem. Phys., 16, 15777–15788,
- 685 https://doi.org/10.5194/acp-16-15777-2016, 2016.

- 687 Chen, Y., Zang, L., Du, W., Xu, D., Shen, G., Zhang, Q., Zou, Q., Chen, J., Zhao, M., and
- Yao, D.: Ambient air pollution of particles and gas pollutants, and the predicted health risks

- from long-term exposure to PM(2.5) in Zhejiang province, China, Environ. Sci. Pollut. Res.
- 690 Int., 25, 23833-23844, DOI:10.1007/s11356-018-2420-5, 2018.

- 692 Cantrell, C. A.: Technical Note: Review of methods for linear least-squares fitting of data and
- application to atmospheric chemistry problems, Atmospheric Chemistry and Physics, 8(17),
- 694 5477–5487, DOI:10.5194/acpd-8-6409-2008, 2008.

695

- 696 Collaud Coen, M., Andrews, E., Bigi, A., Martucci, G., Romanens, G., Vogt, F. P. A., and
- 697 Vuilleumier, L.: Effects of the prewhitening method, the time granularity, and the time
- segmentation on the Mann–Kendall trend detection and the associated Sen's slope, Atmos.
- 699 Meas. Tech., 13, 6945–6964, https://doi.org/10.5194/amt-13-6945-2020, 2020.

700

- 701 Cooke, M.C., Francis, P.N., Millington, S., Saunders, R. and Witham, C.: Detection of the
- 702 Grímsvötn 2011 volcanic eruption plumes using infrared satellite measurements, Atmos. Sci.
- 703 Lett., 15, 321-327, https://doi.org/10.1002/asl2.506, 2011.

704

- 705 Cusack, M., Alastuey, A., Pérez, N., Pey, J., and Querol, X.: Trends of particulate matter
- 706 (PM_{2.5}) and chemical composition at a regional background site in the Western
- Mediterranean over the last nine years (2002–2010), Atmos. Chem. Phys., 12, 8341–8357,
- 708 https://doi.org/10.5194/acp-12-8341-2012, 2012.

709

- 710 Dusek, U., Frank, G. P., Hildebrandt, L., Curtius, J., Schneider, J., Walter, S., Chand, D.,
- 711 Drewnick, F., Hings, S., Jung, D., Borrmann, S., and Andreae, M. O.: Size Matters More
- 712 Than Chemistry for Cloud-Nucleating Ability of Aerosol Particles, Science, 312, 1375-1378,
- 713 DOI:10.1126/science.1125261, 2006.

714

- 715 Flanner, M. G., Gardner, A. S., Eckhardt, S., Stohl, A., and Perket J.: Aerosol radiative
- 716 forcing from the 2010 Eyjafjallajökull volcanic eruptions, J. Geophys. Res. Atmos., 119,
- 717 9481–9491, doi:10.1002/2014JD021977, 2014.

718

- 719 Forsberg, B., Hansson, H.-C., Johansson, C., Areskoug, H., Söderlund, K., and Järvholm, B.:
- 720 Comparative Health Impact Assessment of Local and Regional Particulate Air Pollutants in
- 721 Scandinavia, Ambio, 34, 11-19, 2005.

- 723 Gislason, S., Stefansdottir, G., Pfeffer, M. A., Barsotti, S., Jóhannsson, T., Galeczka, I., Bali,
- 724 E., Sigmarsson, O., Stefansson, A., Keller, N., Sigurdsson, A., Bergsson, B., Galle, B.,
- Jacobo, V. C., Arellano, S., Aiuppa, A., Jonasdottir, E., Eiriksdottir, E., Jakobsson, S., and
- 726 Gudmundsson, M.: Environmental pressure from the 2014–15 eruption of Bárðarbunga
- 727 volcano, Iceland, Geochem. Perspect. Lett., 1, 84-93, DOI:10.7185/geochemlet.1509, 2015.

- 729 Goohs, K., Lilienfeld, P., and Wilbertz, J.: A Synchronized Hybrid Real-Time Particulate
- 730 Monitor, EAC 2009 proceedings, 2009.

731

- Gudmundsson, M. T., Thordarson, T., Höskuldsson, A., Larsen, G., Björnsson, H., Prata, F.
- 733 J., Oddsson, B., Magnússon, E., Högnadóttir, T., Petersen, G. N., Hayward, C. L., Stevenson,
- 734 J. A., and Jónsdóttir, I.: Ash generation and distribution from the April-May 2010 eruption of
- Fyjafjallajökull, Iceland, Scientific reports, 2, 572, https://doi.org/10.1038/srep00572, 2012.

736

- 737 Guenther, A. B., Zimmerman, P. R., Harley, P. C., Monson, R. K., and Fall, R.: Isoprene and
- 738 monoterpene emission rate variability: Model evaluations and sensitivity analyses, Journal of
- 739 Geophys. Res.: Atmos., 98, 12609-12617, DOI:10.1029/93JD00527, 1993.

740

- 741 Guerreiro, C.B.B., Foltescu, V., and de Leeuw, F.: Air quality status and trends in Europe,
- 742 Atmospheric Environment, 98, 376-384, 2014.

743

- Hari, P. and Kulmala, M.: Station for Measuring Ecosystem-Atmosphere Relations: (SMEAR
- 745 II), Boreal Environ. Res., 10, 315-322, DOI:10.1007/978-94-007-5603-8_9, 2005.

746

- 747 Heikkinen, L., Äijälä, M., Riva, M., Luoma, K., Dällenbach, K., Aalto, J., Aalto, P., Aliaga,
- 748 D., Aurela, M., Keskinen, H., Makkonen, U., Rantala, P., Kulmala, M., Petäjä, T., Worsnop,
- 749 D., and Ehn, M.: Long-term sub-micrometer aerosol chemical composition in the boreal
- 750 forest: inter- and intra-annual variability, Atmos. Chem. Phys., 20, 3151-3180,
- 751 DOI:10.5194/acp-20-3151-2020, 2020.

- 753 Heikkinen, L., Äijälä, M., Daellenbach, K. R., Chen, G., Garmash, O., Aliaga, D., Graeffe,
- F., Räty, M., Luoma, K., Aalto, P., Kulmala, M., Petäjä, T., Worsnop, D., and Ehn, M.: Eight
- 755 years of sub-micrometre organic aerosol composition data from the boreal forest

- characterized using a machine-learning approach, Atmos. Chem. Phys., 21, 10081–10109,
- 757 https://doi.org/10.5194/acp-21-10081-2021, 2021.

- 759 Hirsch, R. M., Slack, J. R., and Smith, R. A.: Techniques of trend analysis for monthly water
- 760 quality data, Water Resour. Res., 18, 107–121, DOI:10.1029/WR018i001p00107, 1982.

761

- 762 Ilyinskaya, E., Schmidt, A., Mather, T. A., Pope, F. D., Witham, C., Baxter, P., Jóhannsson,
- 763 T., Pfeffer, M., Barsotti, S., Singh, A., Sanderson, P., Bergsson, B., McCormick Kilbride, B.,
- 764 Donovan, A., Peters, N., Oppenheimer, C., and Edmonds, M.: Understanding the
- 765 environmental impacts of large fissure eruptions: Aerosol and gas emissions from the 2014–
- 766 2015 Holuhraun eruption (Iceland), Earth Planet. Sci. Lett., 472, 309-322,
- 767 DOI:10.1016/j.epsl.2017.05.025, 2017.

768

- 769 IPCC (2021). Climate Change 2021: The Physical Science Basis. Contribution of Working
- 770 Group I to the Sixth Assessment Report of the Intergovernmental Panel on Climate Change.
- 771 Cambridge University Press, Cambridge, United Kingdom and New York, NY, USA, 2021.

772

- Kannosto, J., Virtanen, A., Lemmetty, M., Mäkelä, J. M., Keskinen, J., Junninen, H.,
- Hussein, T., Aalto, P., and Kulmala, M.: Mode resolved density of atmospheric aerosol
- particles, Atmos. Chem. Phys., 8, 5327-5337, DOI:10.5194/acp-8-5327-2008, 2008.

776

- 777 Keskinen, H.-M., Ylivinkka, I., Heikkinen, L., Aalto, P. P., Nieminen, T., Lehtipalo, K.,
- 778 Aalto, J., Levula, J., Kesti, J., Ahonen, L. R., Ezhova, E., Kulmala, M., and Petäjä, T.: Long-
- 779 term aerosol mass concentrations in southern Finland: instrument validation, seasonal
- variation and trends, Atmos. Meas. Tech. Discuss. [preprint], https://doi.org/10.5194/amt-
- 781 2020-447, 2020.

782

- 783 Keuken, M.P., Roemer, M.G.M., Zandveld, P., Verbeek, R.P., and Velders, G.J.M.: Trends in
- 784 primary NO2 and exhaust PM emissions from road traffic for the period 2000-2020 and
- 785 implications for air quality and health in the Netherlands, Atmospheric Environment, 54,
- 786 313-319, 2012.

- 788 Kulkarni, A., and von Storch, H.: Monte Carlo Experiments on the Effect of Serial
- 789 Correlation on the Mann-Kendall Test of Trend Monte Carlo experiments on the effect,
- 790 Meteorologische Zeitschrift, 82–85, DOI:10.1127/METZ/4/1992/82, 1995.

- 792 Kulmala, M., Kontkanen, J., Junninen, H., Lehtipalo, K., Manninen, H. E., Nieminen, T.,
- 793 Petäjä, T., Sipilä, M., Schobesberger, S., Rantala, P., Franchin, A., Jokinen, T., Järvinen, E.,
- 794 Äijälä, M., Kangasluoma, J., Hakala, J., Aalto, P. P., Paasonen, P., Mikkilä, J., Vanhanen, J.,
- Aalto, J., Hakola, H., Makkonen, U., Ruuskanen, T., Mauldin, R. L., Duplissy, J.,
- Vehkamäki, H., Bäck, J., Kortelainen, A., Riipinen, I., Kurtén, T., Johnston, M. V., Smith, J.
- 797 N., Ehn, M., Mentel, T. F., Lehtinen, K. E. J., Laaksonen, A., Kerminen, V.-M., and
- 798 Worsnop, D. R.: Direct Observations of Atmospheric Aerosol Nucleation, Science, 339, 943-
- 799 946, DOI: 10.1126/science.1227385, 2013.

800

- 801 Kulmala, M., Lintunen, A., Lappalainen, H., Virtanen, A., Yan, C., Ezhova, E., Nieminen, T.,
- 802 Riipinen, I., Makkonen, R., Tamminen, J., Sundström, A.-M., Arola, A., Hansel, A.,
- 803 Lehtinen, K., Vesala, T., Petäjä, T., Bäck, J., Kokkonen, T., and Kerminen, V.-M.: Opinion:
- The strength of long-term comprehensive observations to meet multiple grand challenges in
- different environments and in the atmosphere, Atmos. Chem. Phys., 23, 14949–14971,
- 806 https://doi.org/10.5194/acp-23-14949-2023, 2023.

807

- 808 Kyrö, E.-M., Väänänen, R., Kerminen, V.-M., Virkkula, A., Petäjä, T., Asmi, A., Dal Maso,
- 809 M., Nieminen, T., Juhola, S., Shcherbinin, A., Riipinen, I., Lehtipalo, K., Keronen, P., Aalto,
- 810 P. P., Hari, P., and Kulmala, M.: Trends in new particle formation in eastern Lapland,
- 811 Finland: effect of decreasing sulfur emissions from Kola Peninsula, Atmos. Chem. Phys.,
- 812 14(9), 4383–4396, 2014.

813

- Laakso, L., Hussein, T., Aarnio, P., Komppula, M., Hiltunen, V., Viisanen, Y., and Kulmala,
- 815 M.: Diurnal and annual characteristics of particle mass and number concentrations in urban,
- rural and Arctic environments in Finland, Atmos. Environ., 37, 2629-2641, 2003.

- Laakso, L., Laakso, H., Aalto, P. P., Keronen, P., Petäjä, T., Nieminen, T., Pohja, T., Siivola,
- 819 E., Kulmala, M., Kgabi, N., Molefe, M., Mabaso, D., Phalatse, D., Pienaar, K., and
- 820 Kerminen, V. M.: Basic characteristics of atmospheric particles, trace gases and meteorology

- in a relatively clean Southern African Savannah environment, Atmos. Chem. Phys., 8, 4823-
- 822 4839, DOI:10.1016/S1352-2310(03)00206-1, 2008.

- 824 Laj, P., Lund Myhre, C., Riffault, V., Amiridis, V., Fuchs, H., Eleftheriadis, K., Petäjä, T.,
- 825 Salameh, T., Kivekäs, N., Juurola, E., Saponaro, G., Philippin, S., Cornacchia, C., Alados
- 826 Arboledas, L., Baars, H., Claude, A., De Mazière, M., Dils, B., Dufresne, M., Evangeliou, N.,
- 827 Favez, O., Fiebig, M., Haeffelin, M., Herrmann, H., Höhler, K., Illmann, N., Kreuter, A.,
- 828 Ludewig, E., Marinou, E., Möhler, O., Mona, L., Eder Murberg, L., Nicolae, D., Novelli, A.,
- 829 O'Connor, E., Ohneiser, K., Petracca Altieri, R. M., Picquet-Varrault, B., van Pinxteren, D.,
- 830 Pospichal, B., Putaud, J., Reimann, S., Siomos, N., Stachlewska, I., Tillmann, R., Voudouri,
- 831 K. A., Wandinger, U., Wiedensohler, A., Apituley, A., Comerón, A., Gysel-Beer, M.,
- 832 Mihalopoulos, N., Nikolova, N., Pietruczuk, A., Sauvage, S., Sciare, J., Skov, H., Svendby,
- 833 T., Swietlicki, E., Tonev, D., Vaughan, G., Zdimal, V., Baltensperger, U., Doussin, J.,
- 834 Kulmala, M., Pappalardo, G., Sorvari Sundet, S., and Vana, M.: Aerosol, Clouds and Trace
- 835 Gases Research Infrastructure (ACTRIS): The European Research Infrastructure Supporting
- 836 Atmospheric Science, Bulletin of the American Meteorological Society, 105(7), E1098-
- 837 E1136, https://doi.org/10.1175/BAMS-D-23-0064.1, 2024.

838

- 839 Leino, K., Riuttanen, L., Nieminen, T., Dal Maso, M., Väänänen, R., Pohja, T., Keronen, P.,
- 840 Järvi, L., Aalto, P., Virkkula, A., Kerminen, V.-M., Petäjä, T., and Kulmala, M.: Biomass-
- burning smoke episodes in Finland from eastern European wildfires, Boreal Environ. Res.,
- 842 19, 275-292, http://www.borenv.net/BER/pdfs/ber19/ber19B-275.pdf, 2014.

843

- Li X., Li H., Yao L., Stolzenburg D., Sarnela N., Vettikkat L., de Jonge R.W., Baalbaki R.,
- 845 Uusitalo H., Kontkanen J., Lehtipalo K., Daellenback K.R., Jokinen T., Aalto J., Keronen P.,
- 846 Schobesberger S., Nieminen T., Petäjä T., Kerminen V.-M., Bianchi F., Kulmala M., and
- Dada L.: Over 20 years of observations in the boreal forest reveal a decreasing trend of
- atmospheric new particle formation. Boreal Env. Res. 29, 25–52, 2024.

849

- 850 Luoma, K., Virkkula, A., Aalto, P., Petäjä, T., and Kulmala, M.: Over a 10-year record of
- aerosol optical properties at SMEAR II, Atmos. Chem. Phys., 19, 11363–11382,
- 852 https://doi.org/10.5194/acp-19-11363-2019, 2019.

- Luoma, K., Virkkula, A., Aalto, P., Lehtipalo, K., Petäjä, T., and Kulmala, M.: Effects of
- 855 different correction algorithms on absorption coefficient a comparison of three optical
- absorption photometers at a boreal forest site, Atmos. Meas. Tech., 14, 6419–6441,
- 857 https://doi.org/10.5194/amt-14-6419-2021, 2021.

- 859 Lyubovtseva, Y. S., Sogacheva, L., Dal Maso, M., Bonn, B., Keronen, P., and Kulmala, M.:
- 860 Seasonal variations of trace gases, meteorological parameters, and formation of aerosols in
- 861 boreal forests. Boreal Env. Res. 10, 493–510, 2005.

862

- Manavi, S.E.I., Aktypis, A., Siouti, E., Skyllakou, K., Myriokefalitakis, S., Kanakidou, M.,
- 864 Pandis, S.N.: Atmospheric aerosol spatial variability: Impacts on air quality and climate
- 865 change, One Earth 8, 101237, https://doi.org/10.1016/j.oneear.2025.101237, 2025.

866

- Manninen, H., Bäck, J., Sihto-Nissilä, S.-L., Huffman, J., Pessi, A.-M., Hiltunen, V., Aalto,
- P. P., Hidalgo, P., Hari, P., Saarto, A., Kulmala, M., and Petäjä, T.: Patterns in airborne
- pollen and other primary biological aerosol particles (PBAP), and their contribution to
- aerosol mass and number in a boreal forest, Boreal Env. Res., 19 (suppl. B), 383-405, 2014.

871

- 872 Makkonen, U., Virkkula, A., Hellén, H., Hemmilä, M., Sund, J., Äijälä, M., Ehn, M.,
- Junninen, H., Keronen, P., Petäjä, T., Worsnop, D. R., Kulmala, M., and Hakola, H.: Semi-
- 874 continuous gas and inorganic aerosol measurements at a boreal forest site: seasonal and
- diurnal cycles of NH3, HONO and HNO3, Boreal Env. Res., 19 (suppl. B), 311-328, 2014.

876

- 877 Maynard, A. D., and Kuempel, E. D. Airborne Nanostructured Particles and Occupational
- 878 Health. J Nanopart Res 7, 587–614, https://doi.org/10.1007/s11051-005-6770-9, 2005.

879

- 880 Neefjes I., Laapas M., Liu Y., Médus E., Miettunen E., Ahonen L., Quéléver L., Aalto J.,
- Bäck J., Kerminen V-M., Lamplahti J., Luoma K., Mäki M., Mammarella I., Petäjä T., Räty
- 882 M., Sarnela N., Ylivinkka I., Hakala S., Kulmala M., Nieminen T., and Lintunen A.: 25 years
- 883 of atmospheric and ecosystem measurements in a boreal forest Seasonal variation and
- responses to warm and dry years, Boreal Env. Res. 27, 1–31, 2022.

- Neusüß, C., Weise, D., Birmili, W., Wex, H., Wiedensohler, A., and Covert, D. S.: Size-
- 887 segregated chemical, gravimetric and number distribution-derived mass closure of the aerosol

- in Sagres, Portugal during ACE-2, Tellus B: Chem. Phys. Meteorol., 52, 169-184,
- 889 DOI:10.1034/j.1600-0889.2000.00039.x, 2000.

- Niemi, J.V., Saarikoski, S., Aurela, M., Tervahattu, H., Hillamo, R., Westphal, D.L., Aarnio,
- P., Koskentalo, T., Makkonen, U., Vehkamäki, H., and Kulmala, M.: Long-range transport
- 893 episodes of fine particles in southern Finland during 1999–2007, Atmospheric Environment,
- 43, 1255–1264, https://doi.org/10.1016/j.atmosenv.2008.11.022, 2009.

895

- 896 Occhipinti, L. G., and Oluwasanya, P. W.: Particulate Matter Monitoring: Past, Present and
- 897 Future, Int. J. Earth Environ. Sci., 2, 144, doi: https://doi.org/10.15344/2456-351X/2017/144,
- 898 2017.

899

- 900 Pandolfi, M., Alastuey, A., Pérez, N., Reche, C., Castro, I., Shatalov, V., and Querol, X.:
- 901 Trends analysis of PM source contributions and chemical tracers in NE Spain during 2004–
- 902 2014: a multi-exponential approach, Atmos. Chem. Phys., 16, 11787–11805,
- 903 https://doi.org/10.5194/acp-16-11787-2016, 2016.

904

- Peters, T., Ott, D., and O'Shaughnessy, P.: Comparison of the GRIMM 1.108 and 1.109
- 906 Portable Aerosol Spectrometer to the TSI 3321 Aerodynamic Particle Sizer for Dry Particles,
- 907 Ann. Occup. Hyg., 50, 843-850, DOI:10.1093/annhyg/mel067, 2006.

908

- 909 Pope, C., Burnett, R. T., and Thun, M. J.: Lung cancer, cardiopulmonary mortality, and long-
- 910 term exposure to fine particulate air pollution, J. Amer. Med. Assoc., 287, 1132-1141, doi:
- 911 10.1001/jama.287.9.1132, 2003.

912

- 913 Pysarenko, L., Krakovska, S., Savenets, M., Ezhova, E., Lintunen, A., Petäjä, T., Bäck, J. and
- 914 Kulmala, M.: Two-decade variability of climatic factors and its effect on the link between
- 915 photosynthesis and meteorological parameters: example of Finland's boreal forest, Boreal
- 916 Environment Research, 27, 131-144, 2022.

917

- 918 Pöschl, U.: Atmospheric Aerosols: Composition, Transformation, Climate and Health
- 919 Effects, Angewandte Chemie International Edition, 44, 7520-7540,
- 920 https://doi.org/10.1002/anie.200501122, 2005.

- 922 Rantala, P., Taipale, R., Aalto, J., Kajos, M. K., Patokoski, J., Ruuskanen, T. M., and Rinne,
- 923 J.: Continuous flux measurements of VOCs using PTR-MS reliability and feasibility of
- 924 disjunct-eddy-covariance, surface-layer-gradient, and surface-layer-profile methods. Boreal
- 925 Env. Res., 19 (suppl. B), 87–107, 2014.

- 927 Rinne, J., Ruuskanen, T., Reissell, A., Taipale, R., Hakola, H., and Kulmala, M.: On-line
- 928 PTR-MS measurements of atmospheric concentrations of volatile organic compounds in a
- 929 European boreal forest ecosystem, Boreal Environ. Res., 10, 425-436,
- 930 http://www.borenv.net/BER/archive/pdfs/ber10/ber10-425.pdf, 2005.

931

- 932 Riuttanen, L., Hulkkonen, M., Dal Maso, M., Junninen, H., and Kulmala, M.: Trajectory
- analysis of atmospheric transport of fine particles, SO₂, NO_x and O₃ to the SMEAR II station
- 934 in Finland in 1996–2008, Atmos. Chem. Phys., 13, 2153–2164, https://doi.org/10.5194/acp-
- 935 13-2153-2013, 2013.

936

- 937 Saarikoski, S., Mäkelä, T., Hillamo, R., Aalto, P., Kerminen, V.-M., and Kulmala, M.:
- 938 Physicochemical characterization and mass closure of size-segregated atmospheric aerosols
- 939 in Hyytiälä, Finland, Boreal Environ. Res., 10, 386-400, 2005.

940

- 941 Schraufnagel, D.E.: The health effects of ultrafine particles, Exp. Mol. Med., 52, 311–317,
- 942 https://doi.org/10.1038/s12276-020-0403-3, 2020.

943

- 944 Seinfeld, J. and Pandis, S.: Atmospheric chemistry and physics: from air pollution to climate
- 945 change. Second edition. John Wiley & Sons, New Jersey, USA, 2006.

946

- 947 Shiraiwa, M., Ueda, K., Pozzer, A., Lammel, G., Kampf, C. J., Fushimi, A., Enami, S.,
- 948 Arangio, A. M., Fröhlich-Nowoisky, J., Fujitani, Y., Furuyama, A., Lakey, P. S. J., Lelieveld,
- 949 J., Lucas, K., Morino, Y., Pöschl, U., Takahama, S., Takami, A., Tong, H., Weber, B.,
- 950 Yoshino, A., and Sato, K.: Aerosol Health Effects from Molecular to Global Scales,
- 951 Environmental Science & Technology, 51(23), 13545-13567, DOI: 10.1021/acs.est.7b04417,
- 952 2017.

- 954 Shukla, K., and Aggarwal, S.G.: A Technical Overview on Beta-Attenuation Method for the
- 955 Monitoring of Particulate Matter in Ambient Air, Aerosol Air Qual. Res., 22, 220195,
- 956 https://doi.org/10.4209/aaqr.220195, 2022.

- 958 Sicard, P., Agathokleous, E., De Marco, A., Paoletti, E., and Calatayud, V.: Urban population
- exposure to air pollution in Europe over the last decades, Environ. Sci. Eur., 33, 28,
- 960 <u>https://doi.org/10.1186/s12302-020-00450-2</u>, 2021.

961

- 962 Sinclair, V. A., Ritvanen, J., Urbancic, G., Statnaia, I., Batrak, Y., Moisseev, D., and Kurppa,
- 963 M.: Boundary-layer height and surface stability at Hyytiälä, Finland, in ERA5 and
- 964 observations, Atmos. Meas. Tech., 15, 3075–3103, https://doi.org/10.5194/amt-15-3075-
- 965 2022, 2022.

966

- 967 Spindler, G., Müller, K., Brüggemann, E., Gnauk, T., and Herrmann, H.: Long-term size-
- 968 segregated characterization of PM10, PM2.5, and PM1 at the IfT research station Melpitz
- 969 downwind of Leipzig (Germany) using high and low-volume filter samplers, Atmos.
- 970 Environ., 38, 5333-5347, DOI:10.1016/j.atmosenv.2003.12.047, 2004.

971

972 Stull, R. B.: An Introduction to Boundary Layer Meteorology, Springer Dordrecht, 1988.

973

- 974 Stein, A. F., Draxler, R. R., Rolph, G. D., Stunder, B. J. B., Cohen, M. D., and Ngan, F.:
- 975 Noaa's Hysplit Atmospheric Transport and Dispersion Modeling System, B. Am. Meteorol.
- 976 Soc., 96, 2059–2077, https://doi.org/10.1175/BAMS-D-14-00110.1, 2015.

977

- 978 Sui, C., Yu, L., and Vihma, T.: Occurrence and drivers of wintertime temperature extremes in
- 979 Northern Europe during 1979–2016. Tellus A: Dynamic Meteorology and Oceanography,
- 980 72(1), 1–19, https://doi.org/10.1080/16000870.2020.1788368, 2020.

981

- Taipale, R., Ruuskanen, T. M., Rinne, J., Kajos, M. K., Hakola, H., Pohja, T., and Kulmala,
- 983 M.: Technical Note: Quantitative long-term measurements of VOC concentrations by PTR-
- 984 MS measurement, calibration, and volume mixing ratio calculation methods, Atmos. Chem.
- 985 Phys., 8, 6681–6698, https://doi.org/10.5194/acp-8-6681-2008, 2008.

- 987 Tesche, M., Glantz, P., Johansson, C., Norman, M., Hiebsch, A., Ansmann, A., Althausen,
- 988 D., Engelmann, R., and Seifert, P.: Volcanic ash over Scandinavia originating from the
- 989 Grímsvötn eruptions in May 2011, J. Geophys. Res., 117, D09201,
- 990 doi:10.1029/2011JD017090, 2012.

- 992 Thomas, H. E., and Prata, A. J.: Sulphur dioxide as a volcanic ash proxy during the April-
- 993 May 2010 eruption of Eyjafjallajökull Volcano, Iceland, Atmos. Chem. Phys., 11, 6871–
- 994 6880, https://doi.org/10.5194/acp-11-6871-2011, 2011.

995

- 996 Van Dingenen, R., Raes, F., Putaud, J.-P., Baltensperger, U., Charron, A., Facchini, M.,
- 997 Decesari, S., Sandro, F., Gehrig, R., Hansson, H.-C., Harrison, R., Hüglin, C., Jones, A., Laj,
- 998 P., Lorbeer, G., Maenhaut, W., Palmgren, F., Querol, X., Rodriguez, S., and Wåhlin, P.: A
- 999 European aerosol phenomenology 1: Physical characteristics of particulate matter at
- 1000 kerbside, urban, rural and background sites in Europe, Atmos. Environ., 38, 2561-2577,
- 1001 DOI:10.1016/j.atmosenv.2004.01.040, 2004.

1002

- 1003 Viana, M., Kuhlbusch, T.A.J., Querol, X., Alastuey, A., Harrison, R.M., Hopke, P.K.,
- Winiwarter, W., Vallius, M., Szidat, S., Prévôt, A.S.H., Hueglin, C., Bloemen, H., Wåhlin,
- 1005 P., Vecchi, R., Miranda, A.I., Kasper-Giebl, A., Maenhaut, W., and Hitzenberger, R.: Source
- 1006 apportionment of particulate matter in Europe: A review of methods and results, Journal of
- 1007 Aerosol Science, 39, 10, 827-849, https://doi.org/10.1016/j.jaerosci.2008.05.007, 2008.

1008

- 1009 Virkkula, A., Mäkelä, T., Hillamo, R., Yli-Tuomi, T., Hirsikko, A., Hämeri, K., and
- 1010 Koponen, I. K.: A Simple Procedure for Correcting Loading Effects of Aethalometer
- 1011 Data, Journal of the Air & Waste Management Association, 57, 10, 1214–1222,
- 1012 https://doi.org/10.3155/1047-3289.57.10.1214, 2007.

1013

- Waldén, J., Hillamo, R., Aurela, M., Mäkelä, T., and Laurila, S.: Demonstration of the
- 1015 equivalence of PM2.5 and PM10 measurement methods in Helsinki 2007-2008, Studies No.
- 1016 3, Finnish Meteorological Institute, Helsinki, Finland, ISSN 1796-1203, 2010.

- 1018 Wang, W., Chen, Y., Becker, S., and Liu, B.: Linear trend detection in serially dependent
- 1019 hydrometeorological data based on a variance correction Spearman rho method, Water, 7(12),
- 1020 7045–7065, DOI:10.3390/w7126673, 2015.

- 1021
- Wang, J., Xing, J., Mathur, R., Pleim, J. E., Wang, S., Hogrefe, C., Gan, J.-M., Wong, D. C.,
- and Hao, J.: Historical Trends in PM_{2.5}-Related Premature Mortality during 1990–2010
- across the Northern Hemisphere, Environmental Health Perspectives 125, 3,
- 1025 https://doi.org/10.1289/EHP298, 2017.
- 1026
- 1027 WHO global air quality guidelines: Particulate matter (PM2.5 and PM10), ozone, nitrogen
- 1028 dioxide, sulfur dioxide and carbon monoxide, Geneva: World Health Organization, 2021.
- 1029
- 1030 Yli-Juuti, T., Mielonen, T., Heikkinen, L., Arola, A., Ehn, M., Isokääntä, S., Keskinen, H.-
- 1031 M., Kulmala, M., Laakso, A., Lipponen, A., Luoma, K., Mikkonen, S., Nieminen, T.,
- 1032 Paasonen, P., Petäjä, T., Romakkaniemi, S., Tonttila, J., Kokkola, H., and Virtanen, A.:
- 1033 Significance of the organic aerosol driven climate feedback in the boreal area, Nature
- 1034 Communications, 12(1), 1–9, 2021.
- 1035
- 1036 Yttri, K. E., Canonaco, F., Eckhardt, S., Evangeliou, N., Fiebig, M., Gundersen, H.,
- 1037 Hjellbrekke, A.-G., Lund Myhre, C., Platt, S. M., Prévôt, A. S. H., Simpson, D., Solberg, S.,
- 1038 Surratt, J., Tørseth, K., Uggerud, H., Vadset, M., Wan, X., and Aas, W.: Trends, composition,
- and sources of carbonaceous aerosol at the Birkenes Observatory, northern Europe, 2001–
- 1040 2018, Atmos. Chem. Phys., 21, 7149–7170, https://doi.org/10.5194/acp-21-7149-2021, 2021.
- 1041
- 1042 Yue, S., Pilon, P., Phinney, B., and Cavadias, G.: The influence of autocorrelation on the
- ability to detect trend in hydrological series, Hydrol. Process., 16(9), 1807–1829,
- 1044 https://doi.org/10.1002/hyp.1095, 2002.